Journal of Mammalogy, 95(1):9–25, 2014

Cryptic divergence and revised species taxonomy within the Great Basin pocket mouse, *Perognathus parvus* (Peale, 1848), species group

Brett R. Riddle,* Tereza Jezkova, Mallory E. Eckstut, Viktória Oláh-Hemmings, and Leslie N. Carraway

School of Life Sciences, University of Nevada, Las Vegas, 4505 Maryland Parkway, Box 454004, Las Vegas, NV 89154-4004, USA (BRR, TJ, MEE, VO-H)
104 Nash, Department of Fisheries and Wildlife, Oregon State University, Corvallis, OR 97331-3803, USA (LNC)

* *Correspondent: brett.riddle@unlv.edu*

The Great Basin pocket mouse, *Perognathus parvus*, inhabits temperate shrub-steppe and arid grassland biomes throughout the Columbia Plateau, Great Basin, and adjacent regions of western North America. We used both mitochondrial DNA (mtDNA) and nuclear DNA (nDNA) sequences to address phylogenetic and biogeographic structure within the *P. parvus* species group. Phylogenetic and biogeographic analyses divide haplotypes from the mtDNA cytochrome oxidase subunit 3 (COIII) gene into largely allopatric northern versus southern lineages (clades), with divergences of up to 18.8%. The southern mtDNA clade also includes at least 1 of the 2 recently extant populations of the white-eared pocket mouse, *P. alticolus*—an endangered species with a restricted range in southern California. The northern mtDNA clade is further subdivided into several additional lineages with divergences as high as 8.8%, whereas the southern clade has no divergence greater than 1.2%. The deeper mtDNA gene tree structure was recovered by use of nDNA exon sequences from the interphotoreceptor retinoid-binding protein (IRBP) and recombination activating gene 2 (RAG2) gene regions, supporting a "gene tree–species tree" congruence. We estimated through molecular clock analyses that the northern and southern clades likely diverged within a late Miocene time frame. The limited available karyological evidence is consistent with a genome-wide divergence between northern and southern clades—thus, is consistent with recognition of each as a separate species. Conversely, our morphometric analysis revealed a high level of morphological conservatism without detectable diagnostic differences, rendering them as "cryptic" species. We revised species-level taxonomy, designating 2 neotypes given apparent loss of original type specimens. We postulate that barriers associated with Columbia Plateau, Snake River Plain, and Great Basin physiographic evolution, during a Neogene time frame, resulted in persistent geographic isolation driving divergence between the northern and southern clades.

Key words: biogeography, Columbia Plateau, Great Basin, Heteromyidae, mitochondrial DNA, neotype, nuclear DNA, Perognathinae, *Perognathus parvus*, pocket mice

DOI: 10.1644/12-MAMM-A-252

Rodents in the family Heteromyidae represent a diverse assemblage of desert, steppe, and northern tropical taxa with a long evolutionary history in North America (Flynn et al. 2008). They have been used as model organisms for questions ranging from the geography of biotic diversification and assembly of communities to physiological, behavioral, and morphological evolution and the genetics of adaptive evolution (Genoways and Brown 1993; Hoekstra et al. 2004). Many of these studies, however, were conducted prior to molecular investigations that have revolutionized our understanding of heteromyid diversity, including multiple examples of postulated or formally recognized "cryptic" species embedded within morphologically conservative species (Lee et al. 1996; Riddle et al. 2000; McKnight 2005; Hafner et al. 2008; Neiswenter and Riddle 2010, 2011; Rogers and Gonzalez 2010; Hafner and Upham 2011).

Perognathus parvus is a shrub-steppe and arid grassland species distributed across the Columbia Plateau, Colorado Plateau, and Great Basin regions of western North America (Fig. 1). Previous taxonomic treatments considered the yellow-eared pocket mouse as a separate species, *P. xanthonotus* (Williams 1978; Osgood 1900). However, Sulentich (1983)

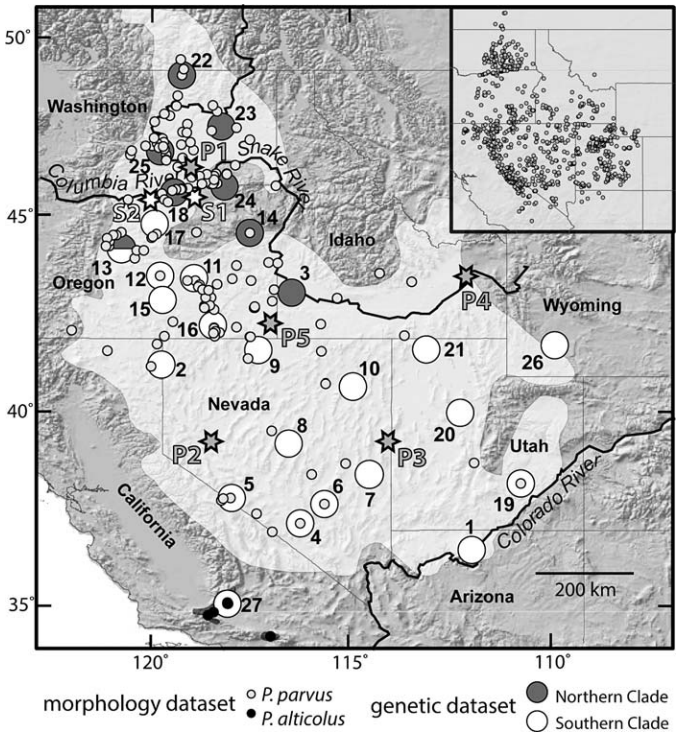

Fig. 1.—General sampling localities (numbered), and distributions of major northern (large dark gray circles) and southern (white circles) clades in the *Perognathus parvus* species group. Morphological samples are shown as smaller gray circles. The locality numbers correspond to those listed in Appendix I and Fig. 2. The inset with small dark gray circles represents known museum records of *P. parvus* and *P. alticolus* downloaded from the MaNIS database. The overall distribution of *P. parvus* is indicated in lighter shading, modified from Hall (1981). Stars represent approximate locations of the fossil sites of the extinct taxon *P. stevei* discussed in the text (S1 = The Dalles, Oregon; S2 = Oregon–Washington state border) and of *P. parvus* (P1 = Jeppson and Kennewick Roadcut sites; P2 = Hidden Cave; P3 = Smith Creek Cave; P4 = Owl Cave; P5 = Dirty Rock Shelter).

used the similarity between chromosomal morphology, allozymes, morphometrics, and phallic morphology to propose that *xanthonotus* be treated as a subspecies within *P. parvus*, and it subsequently has been considered as such (Williams et al. 1993; Wilson and Reeder 2005). Following that revision, the *P. parvus* species group of Osgood (1900) is now composed of 2 species, *P. parvus* and *P. alticolus*. The latter, restricted to enclaves of Great Basin shrub-steppe habitat in the Tehachapi (*P. a. inexpectatus*) and San Bernadino (*P. a. alticolus*) mountains of southern California, is considered an International Union for Conservation of Nature (IUCN) *Red List* endangered species (Linzey and Hammerson 2008), and has been suggested to perhaps be only subspecifically distinct from *P. parvus* (Williams et al. 1993), although we refer to it as a separate species throughout this study.

The *P. parvus* species group comprises a monophyletic clade in relation to 3 additional species groups within the genus according to molecular (Alexander and Riddle 2005; Hafner et al. 2007), morphological (Osgood 1900), and karyological (Williams 1978) evidence. The clade containing *P. parvus* previously was estimated from a molecular phylogenetic analysis to date to about 17–15 million years ago (mya—Hafner et al. 2007). Furthermore, the extinct species *Perognathus stevei*—described from Hemphillian North American Land Mammal Age (about 10–5 mya) specimens in deposits east of The Dalles, Oregon (Carrasco et al. 2005)—was considered similar to extant *P. parvus* (Martin 1984). Geographic ranges of extant species groups in the genus *Perognathus* suggest further that *P. stevei* is an extinct member of the *parvus* species group: 2 (the *longimembris* and *flavus* groups) are residents primarily of warm deserts, grasslands, and steppes far to the south and east of this Columbia Plateau locality; another (the *fasciatus* group) resides in grasslands east of the Rocky Mountains. In combination, molecular phylogenetic, fossil, and geographic evidence suggest a long history of endemism of the *P. parvus* species group in the Columbia Plateau and Great Basin provinces of western North America.

Previous karyological and mitochondrial DNA (mtDNA) studies provided provisional evidence for intraspecific divergence, including presence of at least 2 separate evolutionary lineages, embedded within *P. parvus*. First, Williams (1978) identified marked variation in karyological fundamental number (FN) between individuals representing a Columbia Plateau subspecies (*P. p. columbianus*, diploid number [2N] = 54, FN = 104, X = submetacentric, Y = submetacentric) and 4 subspecies (*P. p. clarus*, *P.p. mollipilosus*, *P. p. olivaceus*, and *P. p. trumbullensis*) from the Basin and Range and Colorado Plateau provinces (2N = 54, FN = 70–76, X = subtelocentric, Y = acrocentric). One or more of the latter 4 subspecies were either identical or similar to specimens of *P. a. inexpectatus* (undifferentiated from *P. p. mollipilosus* and *P. p. olivaceus* from Lassen and Mono counties, California, respectively); and 2 specimens of *P. p. xanthonotus* were undifferentiated from *P. p. clarus* from Duchesne County, Utah.

Second, preliminary studies revealed divergent mtDNA lineages embedded within *P. parvus* (Riddle 1995; Ferrell 1997), but each of those studies had limited geographic sampling that prevented robust estimates of the geographic distribution of lineages. In addition, those mtDNA-only studies were not capable of addressing whether the mtDNA gene tree represented an accurate estimate of species-level divergence history. Herein, we resolve each of these issues by increasing geographic sampling (Fig. 1), and using both mtDNA and nuclear DNA (nDNA) sequences to address phylogenetic and biogeographic structure within the *P. parvus* species group, and propose revision of the nominate species and recognition of a new species. We also use morphometric analyses to address whether groups of populations that are divergent at a molecular level are morphologically diagnosable as well.

Materials and Methods

Genetic samples and laboratory methods.—We collected or acquired 53 tissue samples from 27 sites (Fig. 1; Table 1; Appendix I). These samples included 51 *P. parvus* from 26

sites in 8 states, and 2 samples of *P. a. inexpectatus* from 1 site in the Tehachapi Mountains of California. The San Bernadino Mountains population, *P. a. alticolus*, remains unsampled and could be extinct (Linzey and Hammerson 2008). Samples were collected according to the American Society of Mammalogists guidelines for handling of wild mammals (Sikes et al. 2011) and research was conducted under University of Nevada, Las Vegas, Institutional Animal Care and Use Committee protocol R 0709-244.

We extracted total genomic DNA using the DNeasy extraction kit (Qiagen Inc., Valencia, California) standard protocol. We used primers L8618 and H9323 (Riddle 1995) to amplify and sequence 699 base pairs (bp) of the mtDNA cytochrome oxidase subunit 3 (COIII) gene. We used newly designed primers IRBP_18La (TCA GAC ACT GGC CCA CGT) and IRBP_20H (ACA GAG TCG ATC AGG GCA CT) to amplify the nDNA interphotoreceptor retinoid-binding protein (IRBP) gene, and sequenced 1,062 bp of IRBP using the mentioned primers as well as internal primers 761E and 878F (Jansa and Voss 2000). We used primers R2-283 and R2-1415r (DeBry 2003) to amplify and sequence 1,002 bp of the nDNA recombination activating gene 2 (RAG2) gene. The polymerase chain reactions were run at annealing temperatures of 55°C in 30 cycles (COIII), 55°C in 45 cycles (IRBP), and 52°C in 45 cycles (RAG2) using *Ex Taq* Polymerase Premix (Takara Mirus Bio, Inc., Madison, Wisconsin), and products were purified with ExoSAP-IT (USB Corp., Cleveland, Ohio). We conducted fluorescence-based cycle sequencing for forward and reverse strands using ABI PRISM BigDye Terminator Cycle Sequencing Ready Reaction Kit version 3.1, with electrophoresis on an ABI 3130 automated sequencer (Applied Biosystems, Inc., Foster City, California). We aligned sequences using Sequencher version 4.9 (Gene Codes Corp., Inc., Ann Arbor, Michigan), verified alignments manually, and converted to amino acids to verify open reading frame integrity.

Genetic diversity analyses.—We calculated mean pairwise sequence divergences (uncorrected *p*-distances) using Mega version 5 (Tamura et al. 2011). The IRBP and RAG2 genotypes were converted to haplotypes using the program Phase version 2.1.1 (Stephens and Donnelly 2003), and run for 100 iterations using default parameters. Three replications with a different starting seed yielded consistent data sets.

We imported the COIII, IRBP, and RAG2 data sets to the program Collapse version 1.2 (Posada 2006) to obtain unique haplotypes. We ran the 3 haplotype data sets in jModelTest version 0.1.1 (Posada 2008) to acquire the best-fitting models under the Akaike information criterion (AIC—Posada and Buckley 2004). We conducted maximum-likelihood analyses using the program Treefinder (Jobb et al. 2004), and used the "Bootstrap Analysis" option with 1,000 replicates to build a tree. In MrBayes version 3.2.1 (Ronquist and Huelsenbeck 2003) we ran the COIII haplotype data unpartitioned and partitioned by codon positions (1st + 2nd, 3rd) and applied the Bayes factors method (Nylander et al. 2004). We ran the IRBP and RAG2 haplotype data unpartitioned because of the low variability of the 1st + 2nd codon positions. For the Bayesian inference runs we left the Metropolis-coupled Markov chain Monte Carlo on default. The 50% majority-rule consensus tree and associated posterior probabilities used for final interpretations were based on 3 runs of 5 million generations each. Trees were sampled every 100 generations with the first 25% of sampled trees discarded as burn-in after confirming chain stationarity using the program Tracer version 1.5 (Rambaut and Drummond 2007).

As outgroups (Appendix II), we included *Chaetodipus formosus* as a member of the sister genus to *Perognathus*, with the 2 collectively comprising the subgenus Perognathinae. We also included *P. amplus*, *P. fasciatus*, *P. flavescens*, and *P. longimembris* as representatives from each of 3 species groups (sensu Williams 1978) within *Perognathus* (Alexander and Riddle 2005; Hafner et al. 2007; Neiswenter and Riddle 2010).

Divergence dating.—To estimate the basal divergence of the *P. parvus* species group, as well as divergence of the major clades within this taxon, we obtained sequences from GenBank (Appendix II) for representative heteromyid rodents for cytochrome *b* (*Cytb*; 1,140 bp), COIII (685 bp), and IRBP (1,130 bp), and we generated sequences for RAG2 (1,002 bp). Although *Cytb* was not used in other phylogenetic analyses in this study, *Cytb* sequences were available for a variety of heteromyid rodents in GenBank, allowing us to analyze an additional gene for which we could use fossil calibrations for heteromyids. Inclusion of this range of taxa allowed us to utilize a fossil calibration that previously has been employed in the Heteromyidae and placed as the earliest perognathine fossil at the base of Perognathinae at 22–20 mya (Hafner et al. 2007; Neiswenter and Riddle 2010, 2011). For specimens of *P. parvus*, we used 1 representative per phylogroup as determined in the genetic divergence analyses in this study. We designated 3 taxon groups for analysis as all representatives of the Perognathinae, the genus *Perognathus*, and major clades within the *P. parvus* species group. To examine whether divergence in *P. parvus* resulted from accelerated rates of evolution, we tested for clocklike evolution. We used relaxed clock simulations, where uncorrelated lognormal relaxed clock standard deviation (ucld.stdev) values closer to 0.0 indicate clocklike evolution among lineages and values greater than 1.0 are considered to have heterogeneous rates of evolution among lineages (Drummond et al. 2007).

We estimated divergence times among these heteromyids in the program Beast version 1.7.5 (Drummond and Rambaut 2007). We employed a lognormal prior with a standard deviation of 1 and a relaxed, uncorrelated lognormal clock. We ran simulations with trees linked but unlinked substitution models and clock rates and constrained taxon sets to all Perognathinae (*C. formosus* + all *Perognathus*), all of *Perognathus*, and *P. parvus* clades. All analyses were partitioned by codon (1 + 2 + 3) to account for increased rates of substitution in the 3rd codon position because all genes included are coding regions and thus partitioning by codon is more appropriate for Beast analyses (Drummond et al. 2007). We estimated the most appropriate models of evolution and

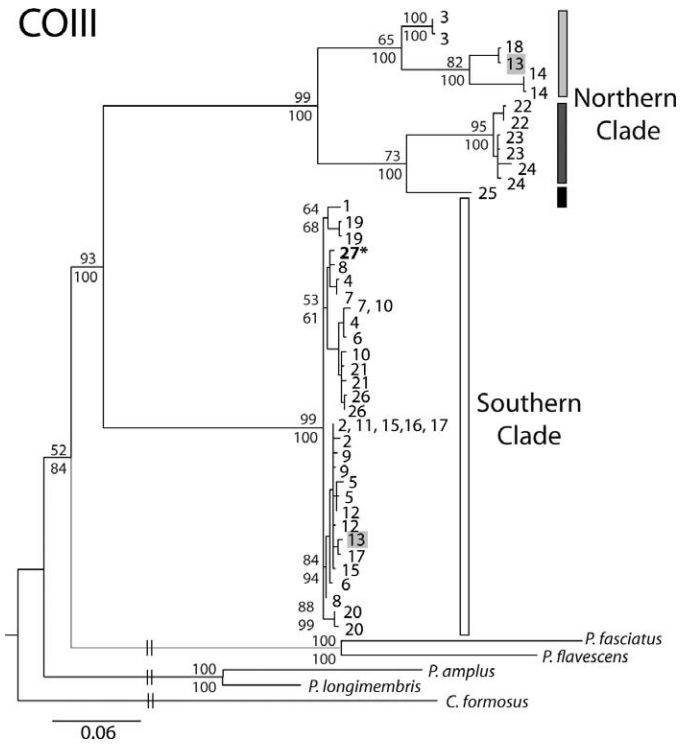

Fig. 2.—Maximum-likelihood tree for 43 unique mitochondrial DNA cytochrome oxidase subunit 3 (COIII) haplotypes of the *Perognathus parvus* species group and 5 outgroup haplotypes. The tip labels represent locality numbers (see Table 1 and Fig. 1) where a particular haplotype was found. The southern clade is bracketed with a white bar; the northern clade is subdivided into 3 subclades (light gray, dark gray, and black bars). A haplotype of *P. alticolus* is indicated with an asterisk (*). The gray rectangle highlights the only locality where co-occurrence of a southern and a northern haplotype was detected. The node labels represent nodal support for the main clades using nonparametric bootstrap values for maximum-likelihood (bootstrap values [BS]; numbers above) and Bayesian inference analyses (posterior probabilities, numbers below). Missing node labels indicate support < 50. Scale bar indicates substitutions per site.

prior parameters using the AIC as implemented in Mega version 5 (Tamura et al. 2011). Because we used 1 representative per taxon or clade, we applied the Yule Process tree prior and ran all analyses 3 times for 10^7 Markov chain Monte Carlo chains that were sampled every 1,000 iterations. We pooled all iterations using Logcombiner version 1.4.8 (Drummond and Rambaut 2007). We imported the resulting log files into Tracer version 1.4.1 (Rambaut and Drummond 2007) and used the effective sample sizes to evaluate the estimates of posterior distributions. The first 10% of generations were discarded as burn-in. We generated the summary of output trees with TreeAnnotator version 1.4.8 (Drummond and Rambaut 2007) and discarded the first 1,000 trees as burn-in.

Morphometric analyses.—For morphometric analyses, we measured 339 specimens, including 325 specimens representing 8 subspecies of *P. parvus*, 10 specimens of *P. a. inexpectatus*, and 4 of *P. a. alticolus* (Appendix I). We divided the specimens of *P. parvus* a priori into groups defined according to genetic analyses in this study. We ran 2 sets of analyses: 1 that treated *P. alticolus* as a separate group, and 1 that included them within one of the genetically defined *P. parvus* groups. All specimens were adults as indicated by tooth wear, reproductive status, condition of pelage, or a combination of these.

For each specimen we recorded total body length, tail length, hind-foot length, and body mass from specimen tags. We measured the following 15 skull and mandible characters with Mitutoyo Digimatic calipers (Mitutoyo America Corp., Aurora, Illinois) to the nearest 0.01 mm: length of skull, skull depth, length of nasals, bulla length, length of upper diastema, length of maxillary toothrow, width of rostrum, zygomatic breadth, least interorbital breadth, cranial breadth, greatest width of interparietal, width between P4 and P4, width between M3 and M3, length of mandible, and length of mandibular toothrow. Statgraphics Centurion XVI version 16.0.03 (StatPoint Technologies, Inc. 2013) was used for all morphometric analyses.

We used principal component analysis (PCA) to compare the genetically delineated groups within *P. parvus* and to compare these groups to *P. alticolus*. We saved factor scores of the first 3 principal components (PCs) and conducted an analysis of variance (ANOVA) on each group to test for group effect. We used discriminant function analysis (DFA) to ascertain the degree to which individuals were assignable to a priori delineated groups within *P. parvus* and to compare these groups to *P. alticolus* (Dillon and Goldstein 1984).

Results

Mitochondrial DNA.—The reduced data set resulted in 43 unique COIII haplotypes within the *P. parvus* species group, plus outgroup haplotypes. jModelTest indicated that the best-fit models were GTR+Γ for the unpartitioned data, and HKY+I (1st + 2nd codon positions) and GTR (3rd codon positions) for the partitioned data. The Bayes factors guided us to choose the partitioned scheme over the unpartitioned scheme for the COIII data set (harmonic mean of the posterior probability distribution for partitioned data = –4,312.33 and unpartitioned data = –4,632.93); however, these models produced similar topologies. Both Bayesian inference and maximum-likelihood analyses resulted in the same general tree structure, split basally into 2 highly distinct and reciprocally monophyletic clades—one with a northern distribution and the other with a southern distribution (hereafter, northern clade and southern clade [Fig. 2]). Within the northern clade ($n = 15$) we detected 13 haplotypes and within the southern clade ($n = 36$) 30 haplotypes.

A unique but not highly divergent haplotype was revealed in *P. alticolus* (haplotype 27 [Fig. 2]). We detected a 13.1% mean pairwise-uncorrected sequence divergence between the northern and southern clades after a standard correction for within-clade diversity (Avise 2000). However, the maximum uncorrected sequence divergence between northern and southern haplotypes was 18.8%. Both clades are divided into several subclades, but with substantially greater divergence in

Table 1.—Samples from the *Perognathus parvus* species group used in the genetics analyses in this study. See Fig. 1 for numbered localities. LVT = Las Vegas Tissue Collection database; MVZ = Museum of Vertebrate Zoology; NMMNH = New Mexico Museum of Natural History; UWBM = University of Washington Burke Museum of Natural History and Culture. A voucher designation of "none" indicates a specimen trapped and released at point of capture. See "*Specimens examined*" (Appendix I) for geographic coordinates and GenBank accession numbers.

Locality no.	State	County	Locality	Sample	Voucher
Perognathus parvus					
1	Arizona	Coconino	House Rock Valley	LVT 9382	None
2	California	Modoc	Eagleville	LVT 8907, 8909	None
3	Idaho	Owyhee	5 mi. W Murphy	LVT 8967, 8968	None
4	Nevada	Nye	36 mi. N, 24 mi. W Mercury	LVT 1805, 1806	NMMNH 3175, 3176
5	Nevada	Esmeralda	11 mi. N, 7 mi. W Dyer	LVT 1931, 1932	NMMNH 3205, 3281
6	Nevada	Lincoln	6 mi. N, 31 mi. W Hiko	LVT 5142, 5143	NMMNH 3880, 3906
7	Nevada	Lincoln	Lake Valley	LVT 7823, 7826	NMMNH 5534, none
8	Nevada	Lander	Monitor Valley	LVT 10173, 10174	None
9	Nevada	Humboldt	Upper Martin Creek, Santa Rosa Mts.	LVT 10208, 10212	None
10	Nevada	Elko	Snow Water Lake	LVT 10378, 10379	None
11	Oregon	Harney	5 mi. S, 4 mi. W Hines	LVT 1925, 1926	NMMNH 3283, 3202
12	Oregon	Lake	2 mi. S, 8 mi. E Hampton	LVT 1943, 1944	NMMNH 3273, 3212
13	Oregon	Jefferson	10 mi. N, 5 mi. E Redmond	LVT 1950, 1951	NMMNH 3215, 3277
14	Oregon	Baker	1 mi. S, 5 mi. E Baker City	LVT 1955, 1958	NMMNH 3279, 3219
15	Oregon	Lake	Alkali Lake	LVT 8932, 8933	None
16	Oregon	Harney	Fields	LVT 8962, 8963	None
17	Oregon	Wheeler	John Day Fossil Beds National Monument	UWBM 77989, 77999	UWBM 77989, 77999
18	Oregon	Morrow	Boardman	LVT 10844, 10846	None
19	Utah	Wayne	9 mi. S, 2 mi. W Hanksville	LVT 1813, 1814	NMMNH 3183, 3184
20	Utah	Tooele	Rush Valley	LVT 8610, 8612	None
21	Utah	Boxelder	Kelton	LVT 8622, 8624	None
22	Washington	Okanogan	4 mi. S, 3 mi. W Oroville	LVT 1953, 1954	NMMNH 3278, 3217
23	Washington	Lincoln		UWBM 77738, 77740	UWBM 77738, 77740
24	Washington	Walla Walla	Whitman Mission National Historic Site	UWBM 77887, 78891	UWBM 77887, 78891
25	Washington	Kittitas	Near Sagebrush Spring	UWBM 78431, 78433	UWBM 78431, 78433
26	Wyoming	Sweetwater	Sweetwater National Wildlife Refuge	LVT 9296, 9297	None
Perognathus alticolus					
27	California	Kern	Cameron Creek, Tehachapi Mts.	MVZ 197331, 197332	MVZ 197331, 197332

the northern clade (a maximum of 8.8% sequence divergence) than in the southern clade (no greater than 1.2% within the southern clade).

The northern clade is distributed primarily north of the Blue Mountains on the Columbia Plateau in northern Oregon and Washington (Fig. 1), but extends at least as far south as locality 3, south of the Snake River in southwestern Idaho. The southern and eastern extent of distribution of the northern clade remains unknown pending further sampling across the majority of the Snake River Plain in Idaho. Locality 13, near Redmond, Oregon, is thus far the only known point of sympatry between northern and southern clades. Subclades within the northern clade appear to be geographically structured, but major river drainages do not appear to form insurmountable barriers (Fig. 1).

Distribution of the southern clade includes the entirety of the Great Basin, the southern portion of the Columbia Plateau in Oregon, the Colorado Plateau in Utah and Arizona, and intermontane basins in western Wyoming (Fig. 1). Samples of *P. a. inexpectatus* at locality 27 are not notably differentiated from southern clade *P. parvus* (Fig. 2), extending the distribution of this clade south at least to the Tehachapi Mountains of southern California. Even though the total geographic expanse of the southern clade far exceeds that of the northern clade, maximum detected sequence divergence was only 1.2% (versus 8.8%).

Nuclear DNA.—For IRBP, the collapsed data set resulted in 33 unique haplotypes and 45 polymorphic sites within the *P. parvus* species group. For RAG2, the collapsed data set resulted in 12 unique haplotypes and 14 polymorphic sites. For both genes, jModelTest chose as the best-fit model HKY+Γ. The general tree structure (including the 2 major clades and 3 subclades within the northern clade) is concordant between the 2 nuclear genes (Fig. 3) and with the mtDNA tree (Fig. 2). Pairwise uncorrected sequence divergences for IRBP and RAG2 between northern and southern clades, corrected for within-clade diversity, are 0.8% and 0.3% (mean); and 1.4% and 0.6% (maximum). Maximum sequence divergences for IRBP and RAG2 within the northern clade are 0.7% and 0.2%, whereas maximum values in the southern clade are 0.4% and 0.2%. Two IRBP haplotypes occurred in *P. alticolus*, 1 unique but not overly divergent and 1 shared with 6 other populations of southern clade *P. parvus* (Fig. 3a). The most frequent RAG2 haplotype in southern clade *P. parvus* also was shared by *P. alticolus* (Fig. 3b).

Divergence dating.—The best-fit models of evolution estimated in Mega version 5 were GTR+I+Γ for COIII, GTR+Γ for *Cytb*, JC for IRBP, and T92 for RAG2. We used

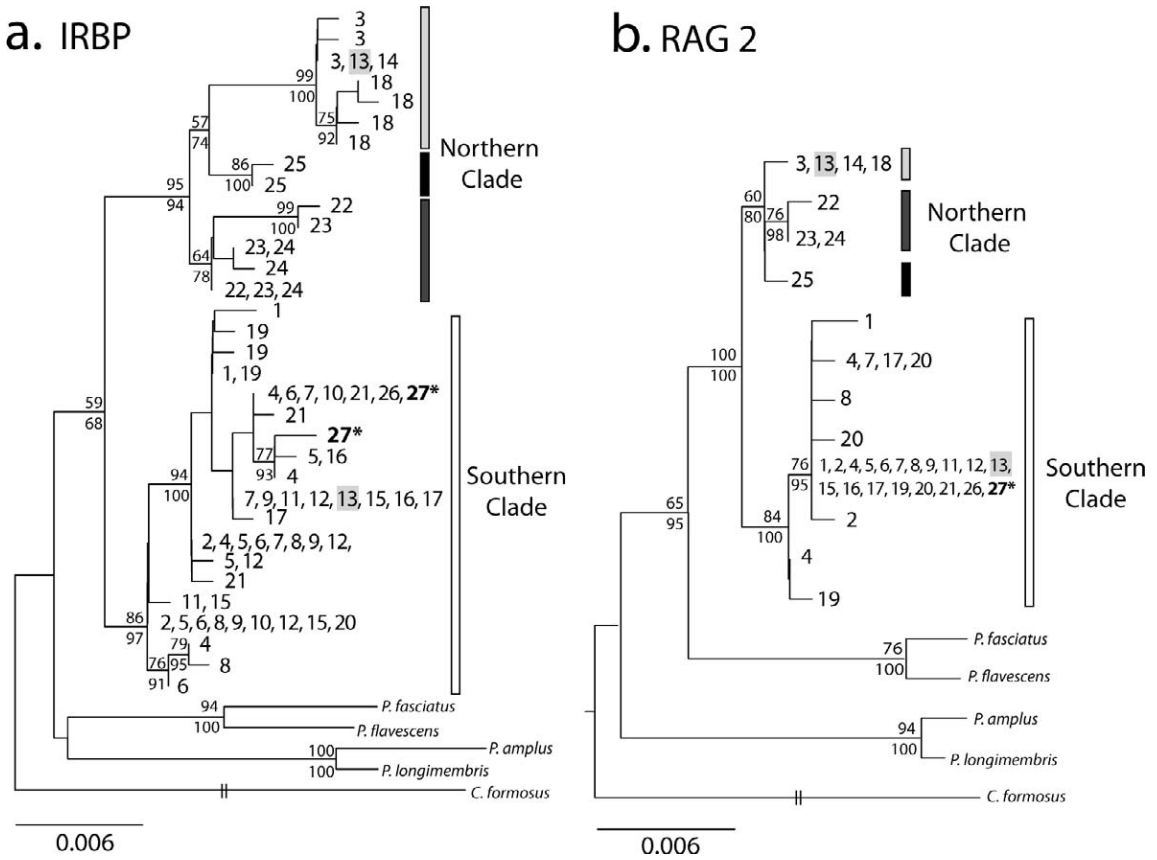

Fig. 3.—Maximum-likelihood trees for a) 33 unique nuclear DNA (nDNA) interphotoreceptor retinoid-binding protein (IRBP) haplotypes, and b) 12 unique nDNA recombination activating gene 2 (RAG2) haplotypes of the *Perognathus parvus* species group, including 5 outgroup haplotypes for each tree. Labeling and nodal values are the same as in Fig. 2. Scale bar indicates substitutions per site.

the models available in the Beast version1.7.5 analyses that were most similar to these (GTR+I+Γ, GTR+Γ, HKY, and HKY, respectively), and effective sample size values were high (> 300), indicating good reliability in the estimates. Deep divergence in *P. parvus* is unlikely to have been the result of accelerated evolution relative to other perognathine clades, because Beast version 1.7.5 revealed relatively clocklike evolution across perognathine clades as indicated by the low standard deviation of the uncorrelated lognormal relaxed clock (ucld.stdev) value (0.19). Nodes on the tree for the 3 designated taxon groups (Fig. 4) placed pooled mean estimates of divergence time at 20.85 mya (range = 22.76–18.85 mya) for the Perognathinae, 19.30 mya (range = 22.25–15.87 mya) for the genus *Perognathus*, and 10.97 mya (range = 14.44–7.37 mya) for the northern versus southern clades of the *P. parvus* species group.

Morphometric analyses.—Specimens of *P. parvus* examined for the morphometric analyses were assigned to the northern or southern groups when they geographically fell within the least-square polygon of genetically identified individuals; the northern group had 191 specimens and the southern group had 108 specimens. Fourteen specimens representing *P. alticolus* were addressed as a separate group even though they fell genetically within the southern group. Twenty-six additional specimens (see Appendix I) that were measured were considered "unsure" (i.e., of unknown genetic designation and falling outside the least-square geographic polygons of the northern and southern groups) and therefore were removed prior to conducting PCAs and DFAs.

The 1st set of analyses was conducted including *P. alticolus* within the southern *P. parvus* clade. The first 3 PCs explained 36.8%, 10.2%, and 8.2% of the total variance, respectively (Appendix II). The ANOVA revealed that PC1 and PC3 significantly differentiate among groups ($P < 0.05$), whereas PC2 does not ($P > 0.05$). However, plotting PC1 against PC3 (Fig. 5A) did not reveal a strong depiction of group separation for northern versus southern groups, nor for *P. alticolus* relative to either of these.

Although the northern and southern groups easily are distinguished based on genetics, DFA of morphometric characters (Appendix IV) resulted in only 86.26% overall separation among the 3 a priori groups (Fig. 5B). For the northern group, 89.01% of specimens were correctly classified into their a priori group. For the southern group, 79.63% of specimens were correctly classified into their a priori group; 4 of the misclassified specimens were classified as *P. alticolus*, but 3 of these were from Oregon and 1 from northern California so can be ruled as not belonging to that species on geographic criteria. All *P. alticolus* were correctly classified into their a priori group. In accord with the nondefinitive rate of

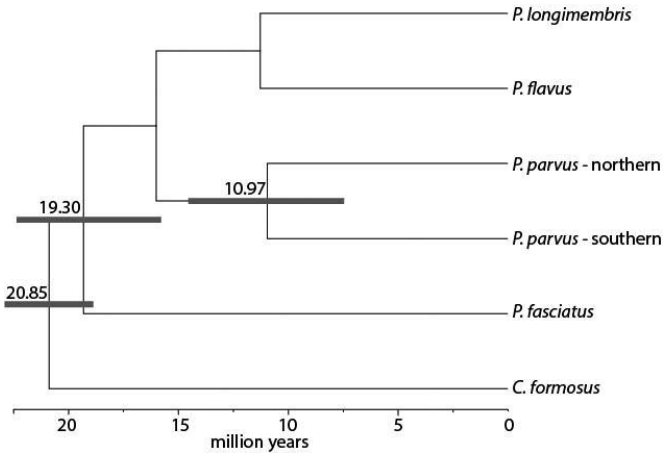

FIG. 4.—Time of divergence estimates for 3 taxon sets as designated for analysis in Beast version 1.7.5. These estimated dates were generated from a concatenated analysis of sequence data from the mitochondrial genes cytochrome oxidase subunit 3 (COIII) and cytochrome *b* (*Cytb*), and nuclear genes interphotoreceptor retinoid-binding protein (IRBP) and recombination activating gene 2 (RAG2). A fossil calibration was placed at the root of the Perognthinae at 22–20 mya (Hafner et al. 2007). Previous molecular phylogenetic analyses (e.g., Alexander and Riddle 2005; Hafner et al. 2007) have been unable to robustly support the sister clade to the *Perognathus parvus* species group, and we are not implying robust support for that specific relationship in this tree.

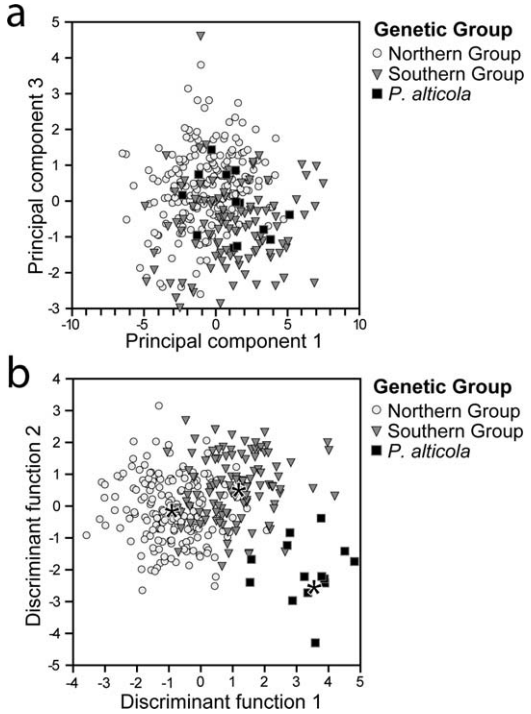

FIG. 5.—A) Scatterplot for principal component 1 and principal component 3 (see Appendix III) derived from 15 cranial and 3 external morphological characters for 323 samples of *Perognathus parvus* assigned a priori to 2 genetic groups (191 northern; 108 southern) and 14 *P. alticolus*. B) Discriminant function plot of 2 genetic groups of *P. parvus* (northern and southern), and *P. alticolus* based on 15 cranial and 3 external characters (see Appendix IV). Asterisks (*) represent group centroids. Discriminant function axis 1 ($\chi^2_{36} = 344.6968$, $P < 0.0001$) accounted for 80.75% and discriminant-function axis 2 ($\chi^2_{17} = 85.0175$, $P < 0.0001$)) accounted for 19.25% of variation present among the 4 groups.

correct classification into their a priori groups, no set of morphological characters was found that could robustly be used to identify specimens of *P. parvus* as belonging to the northern or southern genetic groups. A 2nd set of analyses, treating *P. alticolus* as a 3rd group, differed very little from the 1st.

DISCUSSION

The maximum mtDNA sequence divergence of 18.8% between haplotypes from northern and southern clades in the *P. parvus* species group is noteworthy, and exceeds maximum levels of sequence divergence (mtDNA coding genes *Cytb* or COIII) reported between genetically and geographically separate lineages embedded within other heteromyid species. For example, *Cytb* divergence between 2 lineages in *Microdipodops pallidus* is about 8% (Hafner et al. 2008), whereas that between lineages in *Heteromys desmarestianus* is about 16% (Rogers and Gonzalez 2010). Indeed, this level of divergence exceeds that between 2 morphologically distinct species within *Microdipodops* (*Cytb*, about 13%—Hafner and Upham 2011), and is comparable to that between *P. fasciatus* and the *P. flavescens* and *P. apache* lineage in the *Perognathus fasciatus* species group (COIII, about 18%—Neiswenter and Riddle 2011) and between *P. flavus* and a cryptic southern lineage in the *Perognathus flavus* species group (COIII, about 19%—Neiswenter and Riddle 2010). We provided evidence through a Beast analysis that divergence between northern and southern clades is not likely due to an accelerated rate of evolution relative to other perognathine heteromyids; rather, it probably represents a temporally old lineage divergence within a late Miocene time frame. Questions of interest therefore include landscape evolution that might have driven a lineage divergence of this magnitude, and whether all available sources of evidence warrant recognition of northern and southern clades as separate species.

No molecular-based phylogenies to date (e.g., Alexander and Riddle 2005; Hafner et al. 2007) have provided a robust estimate of the sister clade to the *P. parvus* species group, although all have indicated that both this group and the *P. fasciatus* species group represent separate divergences relative to the well-supported sister-group relationship between the *P. flavus* and *P. longimembris* species groups. We can infer from Hafner et al. (2007:1137, figure 3) that the split between the *P. parvus* species group and other extant *Perognathus* species groups occurred about 17–15 mya. As such, the clade containing the *P. parvus* species group would have existed as a distinct lineage for some 5 million years prior to the split between the extant northern and southern clades.

The estimated origin of the clade containing *P. parvus* at about 17–15 mya (and indeed, the origin of the genus

Perognathus at about 17.6 mya [Hafner et al. 2007]) coincides with topographic and climatic change in western North America. First, the episode of most rapid high-angle block faulting expansion of the Great Basin, and deposition of Columbia Plateau and Snake River Plain basalts (Dickinson 2006), occurred within a time frame of about 17.5–14 mya, creating the topographically more complex landscapes generally associated with episodes of accelerated diversification of mammalian biotas (Kohn and Fremd 2008; Finarelli and Badgley 2010). Second, following the mid-Miocene climatic optimum about 16–15 mya (Zachos et al. 2001), ongoing plateau uplifting in the American West (Colorado Plateau) and Tibet are postulated to have driven a cooling trend and increasing seasonality of climate resulting in a more xeric flora emerging between about 15 and 8 mya (Wing 1998). This shift in biomes would have favored the rapid diversification of granivores, such as most extant perognathine heteromyids, that have the capacity to exploit a higher frequency of seed-producing xeric shrubs and grasses. Additionally, taxa such as the *P. parvus* group would have been capable of entering torpor in more seasonal and cooler climates (French 1993).

The temporal and spatial context of origination of northern versus southern clades in the *P. parvus* species group is consistent with the late Miocene fossil record. The extinct taxon *P. stevei*, described from Hemphillian North American Land Mammal Age specimens in deposits east of The Dalles, Oregon (Fig. 1, star S1; Carrasco et al. 2005), was considered similar to extant *P. parvus* by Martin (1984) in degree of hypsodonty, dentary shape, and several molariform tooth traits, and although differences in traits could be found, he concluded that (p. 104) "none of these differences precludes *P. stevei* from the ancestry of the Recent species [*P. parvus*] . . . ." The Hemphillian North American Land Mammal Age spans about 10–5 mya, placing these specimens near the estimated time of divergence of northern and southern clades. We would postulate based on spatial (Fig. 1) and temporal evidence that *P. stevei* is either a representative of the *P. parvus* clade prior to divergence of the northern and southern clades, or an early representative of the northern clade. In either case, the Miocene location of *P. stevei* at the Oregon–Washington state border and north of the Blue Mountains ecoregion (Fig. 1, star S2; Griffith and Omernik 2009), in connection with evidence from this study of deep lineage divergence of subclades within the northern clade, collectively support the hypothesis that the northern clade has persisted across large expanses of the Columbia Plateau since late Miocene and Pliocene time. The subclades appear to be geographically structured, but more sampling will be required to develop a detailed picture of phylogeographic structure across this region. However, the glacial cycles of the Pleistocene did not appear to have driven populations of the northern clade into a single refugium, which would likely have both reduced intraclade diversity and erased the recovered geographic structuring among subclades.

Northern clade specimens near Murphy, Idaho (locality 3), on the western Snake River Plain appear at 1st somewhat anomalous. However, intermittent connectivity could be postulated via either lower elevation habitat patches within the easternmost Blue Mountains ecoregion habitat mosaic (Griffith and Omernik 2009), for example, in the direction of locality 14; or around the southern edge of this ecoregion, connecting with more western (e.g., locality 13) populations—once again details await more detailed geographic sampling. We suspect that these connections might become more or less restricted in concert with Pleistocene climatic oscillations, and that the relative uniqueness of the mtDNA haplotypes in the vicinity of locality 3 (Fig. 2) result from intermittent episodes of geographic isolation.

There seemingly is more continuous habitat connectivity between locality 3 and localities that are occupied by the southern clade populations to the west, south, and southeast, so it is unclear why locality 3 is not occupied by the southern clade. The detailed phylogeographic structure and analyses that would address the history of the southern clade in these northernmost localities are beyond the scope of this study, but will eventually shed light on this question. Currently, what we can infer is that, in contrast to intraclade structure within the northern clade, haplotype divergence and subclade depth are much shallower within the southern clade, although total numbers of haplotypes are quite high (Fig. 1). This starkly contrasting intraclade structure suggests a profoundly different biogeographic history between northern and southern clades. One possibility would be that, during the Quaternary climatic oscillations, the northern clade retained a widespread geographic distribution and geographic isolation between subclades, whereas the southern clade was purged of haplotype diversity through contractions into 1 or more glacial-age refugia.

The known Glacial or late Wisconsin fossil record (Graham and Lundelius 2010) includes several locality records of interest for *P. parvus*. Jeppson and Kennewick Roadcut sites in Benton County, Washington (Fig. 1, star P1), are both within the current distribution of the northern clade. Hidden Cave in Churchill County (Fig. 1, star P2), and Smith Creek Cave in White Pine County (Fig. 1, star P3), Nevada, are both within the current distribution of the southern clade. At about 10 thousand years ago (kya), fossils in Owl Cave, Bonneville County, Idaho (Fig. 1, star P4), on the far eastern edge of the Snake River Plain, provide evidence for the widespread distribution of *P. parvus* by the end of the Pleistocene. By the late Holocene about 3–2 kya, fossils of *P. parvus* located within the southern clade distribution occur on the southern Columbia Plateau at Dirty Rock Shelter, Malheur County, Oregon (Fig. 1, star P5).

The deep mtDNA genealogical separation between northern and southern lineages in the *P. parvus* species group justifies exploration for ancillary evidence (e.g., from the nuclear genome, morphological differences, etc.) that they represent separate species under application of either a Genetic Species Concept approach as formulated for mammals (Baker and Bradley 2006) or a Genealogical Concordance Species Concept (Avise and Ball 1990). Herein, we have demonstrated concordance between a mitochondrial and 2 nuclear gene trees in the identification of separate southern and northern clades.

Therefore, we argue that all 3 of these gene trees are each tracking the same history of divergence between the 2 clades. Sympatry of both clades at locality 13, and 2 southern clade specimens at locality 17 to the north of locality 13, without demonstrable erosion of nuclear and mitochondrial concordance, provides provisional evidence for recognition of separate species under a Biological Species Concept (Mayr 1942) as well. More sampling at this and other potential contact zones will be required to verify absence of significant hybridization and introgression. However, even if some hybridization occurs between northern and southern lineages, we believe that our overall sampling across the geographic range of the *parvus* species group is sufficient to establish a pervasive historical absence of introgression between northern and southern clades.

We therefore argue that because of a long history of differentiation forming evolutionarily and biogeographically separate mitochondrial and nuclear lineages, the northern and southern clades should be considered as separate species. Because of the absence of diagnostic morphometric differentiation, these species will be difficult or impossible to diagnose from morphological characters, and can be added to a growing list of "cryptic" lineages, some already formally recognized as separate species, of heteromyid rodents (Lee et al. 1996; Riddle et al. 2000; McKnight 2005; Hafner et al. 2008; Neiswenter and Riddle 2010, 2011; Rogers and Gonzalez 2010; Hafner and Upham 2011). Although the northern clade also is subdivided into what appear to be geographically distinct subclades, the current level of geographic sampling and analysis of hybridization is not sufficient to argue for separate species at this level.

The remaining taxonomic issue concerns the status of *P. alticolus*. Examination of available data would argue for inclusion of this taxon within the new southern species given an absence of notable nuclear, mitochondrial, or karyotypic differentiation, although the DFA indicated a relatively clear morphometric differentiation (Fig. 5B). However, 1 of the 2 known sets of allopatric populations (*P. a. alticolus*) remains unsampled, and given that the species is formally designated "endangered" on the *IUCN Red List*, we prefer to retain it as a separate species pending additional sampling.

After thorough search for original holotypes, we believe that both have been lost, and therefore have elected to designate 2 neotypes according to Article 75 of the 4th edition of the *International Code of Zoological Nomenclature* (International Commission on Zoological Nomenclature 1999), and provide formal descriptions below.

Perognathus mollipilosus (Coues, 1875)
Great Basin Pocket Mouse

Perognathus mollipilosus Coues, 1875:296. Type locality "Fort Crook [Shasta County], California."

Perognathus olivaceus Merriam, 1889:15. Type locality "Kelton [near N end Great Salt Lake, Box Elder County], Utah."

Remarks.—Coues (1875) used the name *Perognathus mollipilosus* for a single specimen from Fort Crook, California. This specimen was listed as Holotype 7251 in the National Museum of Natural History (USNM) catalog, an alcohol-preserved female, age unknown, collector J. Feilner, date unknown. According to Fisher and Ludwig (2012), the museum number is incorrect; it is a *Scalopus aquaticus* in the Skin Catalog, and a *Podiceps* in the Bone Catalog. The USNM 7339 catalog entry matches published data for this holotype, but attempts to locate that specimen were unsuccessful (Fisher and Ludwig 2012; A. L. Gardner, USNM, pers. comm.). Osgood (1900) listed 5 specimens from Fort Crook; we therefore chose a representative from this series to represent a neotype for the southern clade. Our choice was based on a high-quality intact specimen, and availability of skin snip material for sequencing of a diagnostic stretch of DNA.

Neotype.—USNM 36760/49145, adult male; California, Shasta County, Fort Crook, 3,000 ft., 41.0°N, 121.44°W.

Diagnosis of neotype.—*Perognathus mollipilosus* is not currently easily distinguishable from *P. parvus* (revised diagnosis) by diagnostic morphological characters (this study). However, it is distinguishable by up to 18.8% mtDNA divergence and 0.8% divergence in 2 nDNA gene sequences (IRBP and RAG2). A short sequence of 44 bp from the mtDNA COIII gene was generated from skin snips removed from the neotype (methods and primers available upon request), and is included here as part of the species diagnosis: GCTCGACAAATTCTCTTCCACTTCACCTCAA CCCACCACTTTGGATTTGAAGCAGCCGCC. This sequence differs by a maximum of 2 mutations from any other *P. mollipilosus* (i.e., southern clade [Fig. 2]), and by 12 mutations from the sequence for the neotype of *P. parvus*.

Description of neotype.—The following external measurements were recorded from specimen tags (in millimeters): total length, 165; tail length, 87; and hind-foot length, 22.0. The following 15 skull and mandible characters were measured to the nearest 0.01 mm: length of skull, 25.10; skull depth, 7.90; length of nasals, 9.79; bulla length, 7.51; length of upper diastema, 5.69; length of maxillary toothrow, 3.47; width of rostrum, 3.96; zygomatic breadth, 11.75; least interorbital breadth, 5.53; cranial breadth, 12.72; greatest width of interparietal, 5.99; width between P4 and P4, 1.77; width between M3 and M3, 2.34; length of mandible, 11.24; and length of mandibular toothrow, 3.13.

The neotype was collected 8 September 1892. Pelage hairs of the dorsum are multibanded. They have black (7.5YR 2/0, where YR = Yellow/Red, 7.5 = the type of Yellow/Red, and 2/0 = the shade of 7.5YR, according to Munsell Color [1975]) tips, a narrow band of very pale brown (10YR 8/4) medially, and a wide band of gray (10YR 5/1) proximally. Hairs of the sides are bicolored with equal lengths of very pale brown (10YR 8/4) distally and gray (10YR 5/1) proximally. Hairs of the venter are all blond-white (10YR 8/1). The tail has a dark dorsal stripe of bicolored hairs with equal lengths of black (7.5YR 2/0) distally and very pale brown (10YR 8/4) proximally for the anterior three-fourths of the tail. For the remaining one-fourth of the distal stripe, the hairs are all gray

(10YR 5/2). The remainder of the tail matches the blond-white of the venter pelage color.

Distribution.—The known distribution of *P. mollipilosus* ranges from central and southern Oregon south and west of the Columbia and Snake rivers, southward through northeastern and south-central California, most of Nevada and Utah west of the Colorado River, southwestern Wyoming, and northern Arizona. Distribution of *P. mollipilosus* overlaps with that of *P. parvus* in 1 examined locality from north-central Oregon (Jefferson County, 10 mi. N, 5 mi. E Redmond). It is currently unknown if *P. mollipilosus* occurs on the central and eastern Snake River Plain in Idaho.

Genetics.—Williams (1978) provided karyological data for 6 female and 1 male specimens from within the geographic range of this species: diploid, 2N = 54; FN = 70–76; X = large subtelocentric; Y = acrocentric. There is less than 1.2% mtDNA haplotype divergence among populations (this study).

Specimens examined.—Total number = 142; genetics = 36; morphology = 108. See Appendix I for locality and accession information.

Perognathus parvus (Peale, 1848)
Columbia Plateau Pocket Mouse

Cricetodipus parvus Peale, 1848:53. Type locality "Oregon," probably near The Dalles, Wasco County (Osgood 1900).

Perognathus parvus Cassin, 1858:48. First use of current name combination.

Perognathus monticola Baird, 1858:422. Type locality "west of Rocky Mountains, St. Marys? [= St. Marys Mission, Stevensville, Montana]"; regarded by Osgood (1900) as having been obtained at The Dalles, Oregon.

Perognathus columbianus Merriam, 1894:263. Type locality "Pasco, Plains of Columbia [Franklin County], Washington (on east side of Columbia river, near mouth of Snake river)."

Perognathus laingi Anderson, 1932:100. Type locality "Anarchist mountain, near Osoyoos-Bridesville summit, about 8 miles east of Osoyoos lake, at about 3,500 feet altitude, latitude 49°08′ north, longitude 119°32′ west [British Columbia, Canada]."

Abromys lordi Gray, 1868:202. Type locality "British Columbia."

Remarks.—Osgood (1900), in his revision of the pocket mice, was unable to locate a type specimen for *P. parvus*, but reasoned from the travels of previous expeditions that it was likely to have been collected at or near The Dalles, Wasco County, Oregon. Cassin (1858) listed the holotype as an alcoholic preserved young female, but neither date of collection nor collector is known. Fisher and Ludwig (2012) indicate that this specimen was part of a United States Exploring Expedition collection that later became part of the USNM. Subsequently, neither Lyon and Osgood (1909) nor Poole and Schantz (1942) listed a representative type specimen. Recent attempts to locate the type at the USNM were unsuccessful (Fisher and Ludwig 2012; A. L. Gardner, USNM, pers. comm.).

We were unable to retrieve genetic samples from specimens collected from the type locality because tissues from available museum specimens were too old and degraded, and collection efforts yielded no specimens because habitat in the vicinity of The Dalles has been substantially altered by agriculture and is now likely unsuitable for *P. parvus*. We therefore chose a representative neotype from a nearby population that represents the geographic distribution of the northern clade. Our choice was based on a high-quality intact specimen, and availability of skin snip material for sequencing of a diagnostic stretch of DNA.

Neotype.—University of Washington Burke Museum of Natural History and Culture (UWBM) 47119, adult male; Washington, Walla Walla County, 3 mi. N, 46.08°N, 118.67°W.

Diagnosis of neotype.—*Perognathus parvus* (revised diagnosis) currently is not easily distinguishable from *P. mollipilosus* by diagnostic morphological characters (this study). It is diagnostic by up to 18.8% mtDNA divergence and 0.8% nDNA divergence in 2 nDNA gene sequences (IRBP and RAG2). A short sequence of 44 bp from the mtDNA COIII gene was generated from skin snips removed from the neotype (methods and primers available upon request), and is included here as part of the species diagnosis: ATCCGAC AAATTCTCTTCCACTTCACTTCCTCTCATCATTTCGGA TTCGAAGCAGCGGCT. This sequence differs by a maximum of 1 mutation from any other *P. parvus* from the subclade in the northern clade that represents localities 22, 23, and 24 (Fig. 2), and by 12 mutations from the sequence for the neotype of *P. mollipilosus*.

Description of neotype.—The following external measurements were recorded from specimen tags (in millimeters or grams): total length, 165; tail length, 93; hindfoot length, 27.0; and body mass, 20. The following 15 skull and mandible characters were measured to the nearest 0.01 mm: length of skull, 24.70; skull depth, 8.42; length of nasals, 9.06; bulla length, 8.91; length of upper diastema, 5.48; length of maxillary toothrow, 3.93; width of rostrum, 4.09; zygomatic breadth, 11.70; least interorbital breadth, 5.42; cranial breadth, 13.00; greatest width of interparietal, 4.74; width between P4 and P4, 1.58; width between M3 and M3, 2.79; length of mandible, 10.50; and length of mandibular toothrow, 3.54.

The neotype was collected 23 July 1974. Pelage hairs of the dorsum are multibanded. They have black (7.5YR 2/0) tips, a very narrow band (1 mm wide) of very pale brown (10YR 8/3) medially, and a wide band of gray (10YR 6/1) proximally. Hairs of the sides are bicolored with equal lengths of very pale brown (10YR 8/3) distally and gray (10YR 6/1) proximally. Hairs of the venter are stark white. The tail has a dark dorsal stripe of scattered short hairs (2 mm) with equal lengths of black (7.5YR 2/0) distally and very pale brown (10YR 8/3) proximally for the anterior three-fourths of the tail. For the remaining one-fourth of the distal stripe, the scattered long hairs (5.5 mm) are all dark grayish-brown (10YR 4/2). The remainder of the tail matches the stark white of the venter pelage color.

Distribution.—The known distribution of *P. parvus* ranges from south-central British Columbia south through central and eastern Washington, northern and northeastern Oregon, and southwestern Idaho along the Snake River. Distribution of *P. parvus* overlaps with that of *P. mollipilosus* in 1 examined locality from north-central Oregon (Jefferson County, 10 mi. N, 5 mi. E Redmond). It is currently unknown if *P. parvus* occurs on the central and eastern Snake River Plain in Idaho.

Genetics.—Williams (1978) provided karyological data for 2 male and 2 female specimens within the geographic distribution of this species: diploid, 2N = 54; autosomal arms, FN = 104; X = submetacentric; Y = submetacentric. There is less than 8.8% mtDNA haplotype divergence among populations (this study).

Specimens examined.—Total number = 202; genetics = 15; morphology = 191. See Appendix I for locality and accession information.

Acknowledgments

We are grateful to A. Ambos, C. Ferrell, A. Jezkova, Z. Deabei, S. Neiswenter, and J. Hafner for assistance with sample collection; and to L. Alexander, A. Francis, and J. Perry for help in the laboratory. We thank the UWBM and Museum of Vertebrate Zoology for providing tissue samples, S. Neiswenter for providing RAG2 sequences for outgroup taxa, and M. Graham for helpful discussions regarding the taxonomic revision. We thank curators and collection managers of the following collections for access to specimens used in morphometric analyses: the Mammal Division, National Museum of Natural History, Washington, D.C.; New Mexico Museum of Natural History; Mammal Collection, Department of Fisheries and Wildlife, Oregon State University; J. R. Slater Museum of Natural History, University of Puget Sound; and UWBM. Extra effort to provide access to specimens chosen to represent neotypes came from J. Bradley at the UWBM; and S. Peurach, N. Woodman, and A. L. Gardner at the USNM—the latter also provided valuable perspective and guidance on taxonomic issues. This work was supported by a University of Nevada, Las Vegas President's Research Award to BRR and J. Jaeger, the National Science Foundation under Cooperative Agreement EPS-0814372 through a National Science Foundation EPSCoR Climate Change Graduate Fellowship and 2 Undergraduate Research Opportunity Fellowships, an American Society of Mammalogists Grant-in-Aid of Research, and a University of Nevada, Las Vegas Graduate and Professional Student Association research grant.

Literature Cited

Alexander, L. F., and B. R. Riddle. 2005. Phylogenetics of the New World rodent family Heteromyidae. Journal of Mammalogy 86:366–379.

Anderson, R. M. 1932. Five new mammals from British Columbia. National Museum of Canada Bulletin 70:99–119.

Avise, J. 2000. Phylogeography: the history and formation of species. Harvard University Press, Cambridge, Massachusetts.

Avise, J., and R. M. Ball, Jr. 1990. Principles of genealogical concordance in species concepts and biological taxonomy. Pp. 45–67 in Oxford surveys in evolutionary biology (D. Futuyma and J. Antonovics, eds.). Oxford University Press, Oxford, United Kingdom.

Baird, S. F. 1857. Mammals. Pp. XXV–XLVIII in Explorations and surveys, to ascertain the most practical and economical route for a railroad from the Mississippi River to the Pacific Ocean. United States Department of the Interior, Washington, D.C. 8:1–157.

Baker, R. J., and R. D. Bradley. 2006. Speciation in mammals and the Genetic Species Concept. Journal of Mammalogy 87:643–662.

Carrasco, M. A., B. P. Kraatz, E. B. Davis, and A. D. Barnosky. 2005. Miocene Mammal Mapping Project (MIOMAP). University of California Museum of Paleontology. http://www.ucmp.berkeley.edu/miomap/. Accessed 22 May 2010.

Cassin, J. 1858. Mammalogy and ornithology. C. Sherman and Son, Philadelphia, Pennsylvania.

Coues, E. 1875. A critical review of North American Sacomyidae. Proceedings of the Academy of Natural Sciences of Philadelphia 27:272–327.

DeBry, R. W. 2003. Identifying conflicting signal in a multigene analysis reveals a highly resolved tree: the phylogeny of Rodentia (Mammalia). Systematic Biology 52:604–617.

Dickinson, W. R. 2006. Geotectonic evolution of the Great Basin. Geosphere 2:353–368.

Dillon, W. R., and M. Goldstein. 1984. Multivariate analysis methods and applications. John Wiley & Sons, Inc., New York.

Drummond, A. J., and A. Rambaut. 2007. Beast: Bayesian evolutionary analysis by sampling trees. BMC Evolutionary Biology 7:214.

Drummond, A. J., S. Y. W. Ho, N. Rawlence, and A. Rambaut. 2007. A rough guide to Beast 1.4. http://beast.bio.ed.ac.uk. Accessed 12 May 2013.

Ferrell, C. 1997. Systematics and biogeography of the Great Basin pocket mouse, *Perognathus paruvs*. M.S. thesis, University of Nevada Las Vegas, Las Vegas.

Finarelli, J. A., and C. Badgley. 2010. Diversity dynamics of Miocene mammals in relation to the history of tectonism and climate. Proceedings of the Royal Society, B. Biological Sciences 277:2721–2726.

Fisher, R. D., and C. A. Ludwig. 2012. Catalog of type specimens of recent mammals: Rodentia (Sciuromorpha and Castorimorpha) in the National Museum of Natural History, Smithsonian Institution. Smithsonian Contributions to Zoology 640:1–97.

Flynn, L. J., E. H. Lindsay, and R. A. Martin. 2008. Geomorpha. Pp. 428–455 in Evolution of Tertiary mammals of North America. Vol. 2: small mammals, xenarthrans, and marine mammals (C. M. Janis, G. F. Gunnell, and M. D. Uhen, eds.). Cambridge University Press, Cambridge, United Kingdom.

French, A. R. 1993. Physiological ecology of the Heteromyidae: economics of energy and water utilization. Pp. 509–538 in Biology of the Heteromyidae (H. H. Genoways and J. H. Brown, eds.). Special Publication 10, The American Society of Mammalogists.

Genoways, H. H., and J. H. Brown (eds.). 1993. Biology of the Heteromyidae. Special Publication 10, The American Society of Mammalogists.

Graham, R. W., and E. L. Lundelius, Jr. 2010. FAUNMAP II: new data for North America with a temporal extension for the Blancan, Irvingtonian and early Rancholabrean. FAUNMAP II database, version 1.0. http://miomap.berkeley.edu/faunmap. Accessed 22 May 2012.

Gray, J. E. 1868. Synopsis of the species of Saccomyinae, or pouched mice, in the collection of the British Museum. Proceedings of the Zoological Society of London 1868:199–206.

Griffith, G. E., and J. M. Omernik (lead authors). 2009. Ecoregions of Oregon (EPA). In Encyclopedia of earth (C. J. Cleveland, M. McGinley, and C. M. Hogan, eds.).Environmental Information Coalition, National Council for Science and the Environment, Washington, D.C. First published in the Encyclopedia of earth

March 17, 2009; last revised date August 9, 2011. http://www.eoearth.org/article/Ecoregions_of_Oregon_(EPA). Accessed 22 May 2012.

Hafner, J. C., et al. 2007. Basal clades and molecular systematics of heteromyid rodents. Journal of Mammalogy 88:1129–1145.

Hafner, J. C., and N. S. Upham. 2011. Phylogeography of the dark kangaroo mouse, *Microdipodops megacephalus*: cryptic lineages and dispersal routes in North America's Great Basin. Journal of Biogeography 38:1077–1097.

Hafner, J. C., N. S. Upham, E. Reddington, and C. W. Torres. 2008. Phylogeography of the pallid kangaroo mouse, *Microdipodops pallidus*: a sand-obligate endemic of the Great Basin, western North America. Journal of Biogeography 35:2102–2118.

Hall, E. R. 1981. The mammals of North America. 2nd ed. John Wiley & Sons, Inc., New York.

Hoekstra, H. E., K. E. Drumm, and M. W. Nachman. 2004. Ecological genetics of adaptive color polymorphism in pocket mice: geographic variation in selected and neutral genes. Evolution 58:1329–1341.

International Commission on Zoological Nomenclature. 1999. International code of zoological nomenclature. 4th ed. International Trust for Zoological Nomenclature, London, United Kingdom.

Jansa, S. A., and R. S. Voss. 2000. Phylogenetic studies on didelphid marsupials I. Introduction and preliminary results from nuclear IRBP gene sequences. Journal of Mammalian Evolution 7:43–77.

Jobb, G., A. von Haeseler, and K. Strimmer. 2004. Treefinder: a powerful graphical analysis environment for molecular phylogenetics. BMC Evolutionary Biology 4:18.

Kohn, M. J., and T. J. Fremd. 2008. Miocene tectonics and climate forcing of biodiversity, western United States. Geology 36:783–786.

Lee, T. E., B. R. Riddle, and P. L. Lee. 1996. Speciation in the desert pocket mouse (*Chaetodipus penicillatus* Woodhouse). Journal of Mammalogy 77:58–68.

Linzey, A. V., and G. Hammerson. 2008. *Perognathus alticolus*. In IUCN 2011, IUCN Red list of threatened species, version 2011.2. www.iucnredlist.org. Accessed 19 May 2012.

Lyon, M. W., Jr., and W. H. Osgood. 1909. Catalogue of the type-specimens of mammals in the United States National Museum, including the biological survey collection. Bulletin of the United States National Museum 62:1–325.

Martin, J. E. 1984. A survey of Tertiary species of *Perognathus* (Perognathinae) and a description of a new genus of Heteromyinae. Special Publications, Carnegie Museum of Natural History 9:90–121.

Mayr, E. 1942. Systematics and the origin of species. Columbia University Press, New York.

McKnight, M. L. 2005. Phylogeny of the *Perognathus longimembris* species group based on mitochondrial cytochrome-*b*: how many species? Journal of Mammalogy 86:826–832.

Merriam, C. H. 1889. Revision of North American pocket mice. North American Fauna 1:1–29.

Merriam, C. H. 1894. Descriptions of eight new pocket mice (genus *Perognathus*). Proceedings of the Academy of Natural Sciences of Philadelphia 46:262–268.

Munsell Color. 1975. Munsell soil color charts. Kollmorgen Corporation, Baltimore, Maryland.

Neiswenter, S. A., and B. R. Riddle. 2010. Diversification of the *Perognathus flavus* species group in emerging arid grasslands of western North America. Journal of Mammalogy 91:348–362.

Neiswenter, S. A., and B. R. Riddle. 2011. Landscape and climatic effects on the evolutionary diversification of the *Perognathus fasciatus* species group. Journal of Mammalogy 92:982–993.

Nylander, J. A. A., F. Ronquist, J. P. Huelsenbeck, and J. L. Nieves Aldrey. 2004. Bayesian phylogenetic analysis of combined data. Systematic Biology 53:47–67.

Osgood, W. H. 1900. Revision of the pocket mice of the genus *Perognathus*. North American Fauna 18:1–72.

Peale, T. R. 1848. United States exploring expedition during the years 1838, 1839, 1840, 1841, 1842. Under the command of Charles Wilkes, U.S.N. Mammalia and ornithology. C. Sherman, Philadelphia, Pennsylvania 8:1–338.

Poole, A. J., and V. S. Schantz. 1942. Catalog of the type specimens of mammals in the United States National Museum, including the biological surveys collection. Bulletin of the United States National Museum 178:1–705.

Posada, D. 2006. Collapse: describing haplotypes from sequence alignment. Computational Evolutionary Biology Lab, University of Vigo, Vigo, Spain.

Posada, D. 2008. jModelTest: phylogenetic model averaging. Molecular Biology and Evolution 25:1253–1256.

Posada, D., and T. R. Buckley. 2004. Model selection and model averaging in phylogenetics: advantages of Akaike information criterion and Bayesian approaches over likelihood ratio tests. Systematic Biology 53:793–808.

Rambaut, A., and A. J. Drummond. 2007. Tracer (version 1.54) [computer software]. http://beast.bio.ed.ac.uk/Tracer. Accessed 12 May 2012.

Riddle, B. R. 1995. Molecular biogeography in the pocket mice (*Perognathus* and *Chaetodipus*) and grasshopper mice (*Onychomys*): the late Cenozoic development of a North American aridlands rodent guild. Journal of Mammalogy 76:283–301.

Riddle, B. R., D. J. Hafner, and L. F. Alexander. 2000. Comparative phylogeography of Baileys' pocket mouse (*Chaetodipus baileyi*) and the *Peromyscus eremicus* species group: historical vicariance of the Baja California Peninsular desert. Molecular Phylogenetics and Evolution 17:161–172.

Rogers, D. S., and M. W. Gonzalez. 2010. Phylogenetic relationships among spiny pocket mice (*Heteromys*) inferred from mitochondrial and nuclear sequence data. Journal of Mammalogy 91:914–930.

Ronquist, F., and J. P. Huelsenbeck. 2003. MrBayes 3: Bayesian phylogenetic inference under mixed models. Bioinformatics 19:1572–1574.

Sikes, R. S., W. L. Gannon, and the Animal Care and Use Committee of the American Society of Mammalogists. 2011. Guidelines of the American Society of Mammalogists for the use of wild mammals in research. Journal of Mammalogy 92:235–253.

StatPoint Technologies, Inc. 2013. Statgraphics Centurion XVI. Version 16. StatPoint Technologies, Inc, Warrenton, Virginia.

Stephens, M., and P. Donnelly. 2003. A comparison of Bayesian methods for haplotype reconstruction from population genotype data. American Journal of Human Genetics 73:1162–1169.

Sulentich, J. M. 1983. The systematics and evolution of the *Perognathus parvus* species group in southern California (Rodentia: Heteromyidae). M.S. thesis, California State University, Long Beach.

Tamura, K., D. Peterson, N. Peterson, G. Stecher, M. Nei, and S Kumar. 2011. Mega5: molecular evolutionary genetics analysis using maximum likelihood, evolutionary distance, and maximum parsimony methods. Molecular Biology and Evolution 28:2731–2739.

Williams, D. F. 1978. Karyological affinities of species groups of silky pocket mice (Rodentia, Heteromyidae). Journal of Mammalogy 59:599–612.

Williams, D. F., H. H. Genoways, and J. K. Braun. 1993. Taxonomy. Pp. 38–196 in Biology of the Heteromyidae (H. H. Genoways and J. H. Brown, eds.). Special Publication 10, The American Society of Mammalogists.

Wilson, D. E., and D. M. Reeder (eds.). 2005. Mammal species of the world: a taxonomic and geographic reference. 3rd ed. Johns Hopkins University Press, Baltimore, Maryland.

Wing, S. L. 1998. Tertiary vegetation of North America as a context for mammalian evolution. Pp. 37–60 in Evolution of tertiary mammals of North America (C. M. Janis, K. M. Scott, and L. L. Jacobs, eds.). Cambridge University Press, New York.

Zachos, J., M. Pagani, L. Sloan, E. Thomas, and K. Billups. 2001. Trends, rhythms, and aberrations in global climate 65 Ma to present. Science 292:686–693.

Submitted 27 September 2012. Accepted 22 September 2013.

Associate Editor was Burton K. Lim.

Appendix I

Specimens examined.— Specimens are housed in the following collections: Museum of Vertebrate Zoology (MVZ), New Mexico Museum of Natural History (NMMNH), Oregon State University (OSUFW), University of Puget Sound (PSM), National Museum of Natural History (USNM), University of Washington Burke Museum of Natural History and Culture (UWBM), and City of Rocks National Reserve (CIRO). Specimens without vouchers that were used for genetic analysis are deposited in the University of Nevada, Las Vegas Tissue Collection (LVT). Specimens used in morphological analyses are designated with an "m" and those used in the molecular analyses are designated with an "M." Following indicated use in molecular analysis, we also include tissue sample number (if different from voucher number) and GenBank accession numbers. GenBank accession numbers for molecular analyses are listed for specimens in the following order: cytochrome oxidase subunit 3 (COIII), interphotoreceptor retinoid-binding protein (IRBP) allele 1, IRBP allele 2, recombination activating gene 2 (RAG2) allele 1, and RAG2 allele 2. Country, state, county, and locality are listed in alphabetical order by species. Specimens are grouped and listed according to the revised species taxonomy proposed in this study.

Perognathus alticolus (m = 14; M = 2).—***UNITED STATES: California;*** *Kern County;* Cameron Creek, Tehachapi Mts. (35.09°, –118.31°), MVZ197329 (m), MVZ197331 (M, KF382742, KF382795, KF382796, KF382901, KF382902), MVZ197332 (M, KF382743, KF382797, KF382798, KF382903, KF382904); Bronco Canyon, Tehachapi Mts. (34.87°, –118.68°), MVZ196745 (m); 3 mi. E Monolith (35.12°, –118.32°), PSM08868 (m), PSM08870 (m), PSM08861 (m), PSM08872 (m); 0.5 mi. SW Cameron (35.09°, –118.31°), MVZ125995 (m), MVZ125997 (m), MVZ125998 (m); *Los Angeles County;* 2 mi. E Gorman (34.78°, –118.82°), MVZ096542 (m); *San Bernadino County;* 2 mi. E Strawberry Peak (34.23°, –117.20°), MVZ047408 (m), MVZ047409 (m), MVZ047411 (m), MVZ047416 (m)

Perognathus mollipilosus (m = 108; M = 36).—***UNITED STATES: Arizona;*** *Coconino County;* House Rock Valley (36.49°, –111.96°), LVT9381 (M, KF382744, KF382799, KF382800, KF382905, KF382906); ***California;*** *Modoc County;* Eagleville (41.32°, –120.04°), LVT8906 (M, KF382745, KF382801, KF382802, KF382907, KF382908), LVT8909 (M, KF382746, KF382803, KF382804, KF382909, KF382910); 0.5 mi. SE Lava Beds National Monument, T44N, R5E, Sec. 6, 4,300 ft (41.68°, –121.44°), PSM24431 (m); Fort Bidwell (41.86°, –120.15°), PSM10740 (m); Jess Valley, 14 mi. E Likely (41.27°, –120.30°), PSM10751 (m); *Mono County;* Benton Station, 1.25 mi. N, 2.5 mi. E, 6,900 ft (37.84°, –118.43°), UWBM47039 (m); Benton, 3 mi. S (37.78°, –118.48°), UWBM47018 (m); *Shasta County;* Fort Crook, 3,000 ft (41.00°, –121.44°), USNM 36760/49145 (m); ***Idaho;*** *Blaine County;* Sun Valley, (43.70°, –114.35°), PSM03936 (m); Arco, 16 mi. SW, Craters of the Moon National Monument, NE entrance, 5,880 ft (43.47°, –113.53°), UWBM50493 (m); *Cassia County;* [CIRO 1751], City of Rocks National Reserve, Transect 03, 1,970 m (42.14°, –118.68°), UWBM78897 (m); [CIRO 1752], City of Rocks National Reserve, Transect 34, 1,896 m (42.08°, –113.70°), UWBM78913 (m); [CIRO 1762], City of Rocks National Reserve, Transect 35, 2,033 m (42.08°, –113.70°), UWBM78901 (m); [CIRO 1770], City of Rocks National Reserve, 1,887 m (42.08°, –113.70°), UWBM79667 (m); [CIRO 1773], City of Rocks National Reserve, 1,828 m (42.08°, –113.70°), UWBM79670 (m); [CIRO 1781], City of Rocks National Reserve, 1,868 m (42.08°, –113.70°), UWBM79665 (m); [CIRO 1796], City of Rocks National Reserve, 1,837 m (42.08°, –113.70°), UWBM79668 (m); *Elmore County;* Hammett, 6 mi. N (43.03°, –115.47°), UWBM47075 (m); Hammett, 7 mi. N (43.05°, –115.47°), UWBM47077 (m), UWBM47080 (m), UWBM47082 (m), UWBM47085 (m); *Owyhee County;* Grasmere, 5,200 ft (42.38°, –115.88°), PSM07572 (m), PSM07573 (m), PSM07574 (m), PSM07575 (m), PSM07586 (m), PSM07587 (m); ***Nevada;*** *Elko County;* 12 mi. S, 5.5 mi. E Mountain City (41.66°, –115.87°), NMMNH3269 (m); Elko (40.83°, –115.76°), USNM024418 (m); Snow Water Lake (40.75°, –115.05°), LVT10378 (M, KF382747, KF382805, KF382806, KF382911, KF382912), LVT10379 (M, KF382748, KF382807, KF382808, KF382913, KF382914); *Esmeralda County;* 11 mi. N, 7 mi. W Dyer, T1S, R34E, S1/2 NE1/4 Sec. 19, 7,100 ft (37.84°, –118.24°), NMMNH3207 (m), NMMNH3205 (m; M, LVT1931, KF382749, KF382809, KF382810, KF382915, KF382916), NMMNH3206 (m), NMMNH3281 (M, LVT1932, KF382750, KF382811, KF382812, KF382917, KF382918); 11 mi. N, 7 mi. W Dyer, T1S, R34E, Sec. 19, ca. 7,100 ft (37.84°, –118.24°), NMMNH3281 (m); Mt. Magruder (37.44°, –117.56°), USNM028422 (m), USNM028423 (m), USNM028425 (m), USNM028905 (m); *Humboldt County;* 35 mi. N, 2 mi. W Winnemucca (41.48°, –117.77°), NMMNH3332 (m), NMMNH3331 (m), NMMNH3330 (m); Upper Martin Creek, Santa Rosa Mts. (41.69°, –117.51°), LVT10208 (M, KF382751, KF382813, KF382814, KF382919, KF382920), LVT10212 (M, KF382752, KF382815, KF382816, KF382921, KF382922); *Lander County;* Monitor Valley (39.26°, –116.72°), LVT10173 (M, KF382753, KF382817, KF382818, KF382923, KF382924), LVT10174 (M, KF382754, KF382819, KF382820, KF382925, KF382926); Reese River (39.59°, –117.16°), USNM024959 (m), USNM024962 (m), USNM024965 (m); *Lincoln County;* 6 mi. N, 31 mi. W Hiko, 4,800 ft (37.69°, –115.79°), NMMNH3878 (m), NMMNH3879 (m), NMMNH3904 (m), NMMNH3880 (m; M, LVT5142, KF382755, KF382821, KF382822, KF382927, KF382928); NMMNH3906 (M, LVT5143, KF382756, KF382823, KF382824, KF382929, KF382930); Lake Valley (38.46°, –114.62°), NMMNH5534 (M, LVT7823, KF382757, KF382825, KF382826, KF382931, KF382932), LVT7826 (M, KF382758, KF382827, KF382828, KF382933, KF382934); *Nye County;* Currant, 13 mi. E (38.74°, –115.23°), UWBM47007 (m), UWBM47008 (m), UWBM47010 (m); Grapevine Mts., 5,500 ft (36.97°, –117.15°), USNM028829 (m); 19.2 mi. N, 14 mi. E Warm Springs, 6,030 ft (38.47°, –116.13°), NMMNH3545 (m), NMMNH3546 (m); 36 mi. N, 24 mi. W Mercury on Buckboard Mesa Rd., 5,600 ft (37.18°, –116.43°), NMMNH3175 (m; M, LVT1805, KF382759, KF382829, KF382830, KF382935, KF382936), NMMNH3176 (m; M, LVT1806, KF382760, KF382831, KF382832, KF382937, KF382938); ***Oregon;*** *Crook County;* Prineville, 17 mi. E (44.30°, –120.49°), UWBM60825 (m); 13.5 mi. S, 2.5 mi. E Prineville, 3,500 ft (44.12°, –120.80°), OSUFW1648 (m); Prineville, 2,877 ft (44.30°, –120.83°),

USNM207358 (m), USNM207359 (m); *Deschutes County;* 2 mi. S, 8 mi. E Hampton, T22S, R21E (43.64°, –120.07°), NMMNH3214 (m), NMMNH3213 (m), NMMNH3273 (m), NMMNH3275 (m); *Harney County;* Fields (42.31°, –118.66°), LVT8962 (M, KF382761, KF382833, KF382834, KF382939, KF382940), LVT8963 (M, KF382762, KF382835, KF382836, KF382941, KF382942); Fields, 0.3 mi. S on Fields–Denio Rd, ~1,249 m (42.27°, –118.67°), UWBM74566 (m), UWBM74567 (m), UWBM74569 (m); Fields, 4.6 mi. S, along Fields–Denio Rd., 1,268 m (42.19°, –118.63°), UWBM78515 (m); Fields, 5.7 mi. S, 0.5 mi. W near Willow Creek, 1,280 m (42.19°, –118.63°), UWBM78512 (m); 1.5 mi. N Fields (42.28°, –118.67°), OSUFW6870 (m); 12 mi. S, 15 mi. W Burns (43.51°, –119.35°), OSUFW8201 (m); 16.5 mi. N, 1.5 mi. E Frenchglen, T29S, R31E, SE1/4 Sec. 9 (43.07°, –118.88°), OSUFW7439 (m); 17.5 mi. N, 1.5 mi. E Frenchglen, T29S, R31E, SE1/2 Sec. 4 (43.08°, –118.88°), OSUFW7431 (m); 2 mi. N, 4 mi. E Frenchglen, Malheur NWR, 4,200 ft (42.85°, –118.91°), OSUFW3001 (m); 23 mi. S, 5.5 mi. W Burns, NW shore Harney Lake, 4,200 ft (43.36°, –119.07°), OSUFW2941 (m); 42 mi. S, 12 mi. E Burns, Malheur NWR, 4,200 ft (43.07°, –118.75°), OSUFW2943 (m); 5 mi. N Denio (42.06°, –118.64°), USNM247779 (m), USNM247780 (m); 5 mi. N, 4 mi. W Hines, T24S, R30E, Sec. 8 (43.51°, –119.15°), NMMNH3201 (m), NMMNH3200 (m), NMMNH3202 (M, LVT1926, KF382763, KF382837, KF382838, KF382943, KF382944), NMMNH3203 (m), NMMNH3283 (M, LVT1925, KF382764, KF382839, KF382840, KF382945, KF382946); 6 mi. E Frenchglen, T32S, R32.5E, Sec. 14 (42.82°, –118.77°), OSUFW4301 (m); 6.75 mi. S, 12 mi. E Fields, T39S, R36E, Sec. 25 (42.16°, –118.53°), OSUFW6868 (m), OSUFW6869 (m); Crane, 4,134 ft (43.42°, –118.58°), USNM215922 (m); Narrows (43.27°, –118.97°), USNM216166 (m); Steens Mt., T31S, R32.5E, Sec. 23 (42.86°, –118.78°), OSUFW4319 (m); Steens Mt., T31S, R32.5E, Sec. 3 (42.91°, –118.85°), OSUFW4298 (m), OSUFW4315 (m); Steens Mt., T32S, R32.75E, Sec. 36 (42.75°, –118.67°), OSUFW4318 (m); Steens Mt., T32S, R32E, Sec. 10 (42.80°, –118.92°), OSUFW4320 (m); Voltage, 4,111 ft (43.26°, –118.81°), USNM235052 (m); *Jackson County;* Howard Prairie Reservoir, 1 mi. N, T38S, R3E, Sec. 13 NE1/4 (42.22°, –122.38°), PSM24433 (m); *Jefferson County;* 10 mi. N, 5 mi. E Redmond (44.42°, –121.07°), NMMNH3277 (M, LVT1951, KF382765, KF382841, KF382842, KF382947, KF382948); *Lake County;* 2 mi. S, 8 mi. E Hampton (43.64°, –120.07°), NMMNH3273 (M, LVT1943, KF382766, KF382843, KF382844, KF382949, KF382950), NMMNH3212 (M, LVT1944, KF382767, KF382845, KF382846, KF382951, KF382952); 20 mi. NE Adel, Hart Mt., site of Old Camp Warner (42.43°, –119.73°), OSUFW6549 (m), OSUFW6550 (m); Adel, Twentymile Creek (42.06°, –119.95°), OSUFW6551 (m), OSUFW6546 (m), OSUFW6547 (m), OSUFW6548 (m); Alkali Lake (43.01°, –120.01°), LVT8932 (M, KF382768, KF382847, KF382848, KF382953, KF382954), LVT8933 (M, KF382769, KF382849, KF382850, KF382955, KF382956); *Malheur County;* 3 mi. N McDermitt, NV (42.04°, –117.73°), PSM06111 (m); 3 mi. N McDermitt, NV (42.04°, –117.72°), PSM06110 (m); Jordan Valley, 5 mi. W (42.97°, –117.15°), PSM06127 (m); Whitehorse Ranch, 6.5 mi. SE, T38S, R39E, Sec. 1, E1/2 (42.30°, –118.08°), PSM23867 (m); 24 mi. S, 2 mi. E Burns, Malheur NWR, Sec. 21, S end Mud Lake (43.40°, –119.040°), OSUFW1642 (m); 3 mi. S Rome, Owyhee Canyon, 3,500 ft (42.80°, –117.62°), OSUFW0575 (m), OSUFW0576 (m); 3 mi. S, 1 mi. E Rome, 3,500 ft (42.80°, –117.60°), OSUFW1626 (m); Rome, Owyhee River (42.83°, –117.61°), USNM207892 (m); *Wheeler County;* John Day Fossil Beds N. M., 682 m (44.63°, –120.29°), UWBM77989 (m; M, KF382770, KF382851, KF382852, KF382957, KF382958); John Day Fossil Beds N. M., 727 m (44.66°, –120.26°), UWBM77999 (m; M, KF382771, KF382853, KF382854, KF382959, KF382960); Twickenham (44.73°, –120.16°), USNM209632 (m), USNM209637 (m); ***Utah;*** *Boxelder County;* Kelton (41.72°, –113.14°), LVT8622 (M, KF382772, KF382855, KF382856, KF382961, KF382962), LVT8624 (M, KF382773, KF382857, KF382858, KF382963, KF382964); *Sevier County;* Richfield, 10 mi. E, 6,550 ft (38.77°, –111.90°), UWBM46977 (m); *Tooele County;* Rush Valley (40.08°, –112.26°), LVT8609 (M, KF382774, KF382859, KF382860, KF382965, KF382966), LVT8612 (M, KF382775, KF382861, KF382862, KF382967, KF382968); *Wayne County;* 9 mi. S, 2 mi. W Hanksville, T30S, R11E, Sec. 2 (38.23°, –110.69°), NMMNH3183 (m; M, LVT1813, KF382776, KF382863, KF382864, KF382969, KF382970), NMMNH3184 (m; M, LVT1814, KF382777, KF382865, KF382866, KF382971, KF382972), NMMNH3185 (m), NMMNH3186 (m); ***Wyoming;*** *Sweetwater County;* Sweetwater NWR (41.82°, –109.80°), LVT9296 (M, KF382778, KF382867, KF382868, KF382973, KF382974), LVT9297 (M, KF382779, KF382869, KF382870, KF382975, KF382976)

Perognathus parvus (m = 191; M = 15).—***CANADA: British Columbia;*** Vaseaux Lake (49.28°, –119.53°), PSM07570 (m); Yale District, Osoyoos, 1,500 ft (49.03°, –119.45°), PSM03084 (m), PSM03083 (m); ***UNITED STATES: Idaho;*** *Owyhee County;* 5 mi. W Murphy (43.19°, –116.64°), LVT8966 (M, KF382780, KF382871, KF382872, KF382977, KF382978), LVT8968 (M, KF382781, KF382873, KF382874, KF382979, KF382980); ***Oregon;*** *Baker County;* 1 mi. S, 5 mi. E Baker City, T9S, R40E (44.76°, –117.73°), NMMNH3279 (m; M, LVT1955, KF382782, KF382875, KF382876, KF382981, KF382982), NMMNH3218 (m), NMMNH3219 (m; M, LVT1958, KF382783, KF382877, KF382878, KF382983, KF382984); *Gilliam County;* Willows (45.79°, –120.02°), USNM206699 (m), USNM206704 (m), USNM206705 (m), USNM206707 (m), USNM206708 (m), USNM206709 (m); *Jefferson County;* 10 mi. N, 5 mi. E Redmond (44.42°, –121.07°), NMMNH3215 (M, LVT1950, KF382784, KF382879, KF382880, KF382985, KF382986); *Malheur County;* 5 mi. SW Ontario, Wood Ranch, 2,000 ft (43.97°, –117.00°), USNM211580 (m); Vale, 2,244 ft (43.98°, –117.24°), USNM207901 (m); *Morrow County;* Boardman (45.81°, –119.71°), LVT10844 (M, KF382785, KF382881, KF382882, KF382987, KF382988), LVT10846 (M, KF382786, KF382883, KF382884, KF382989, KF382990); Cecil, McIntyre Camp (45.62°, –119.96°), PSM07564 (m), PSM07565 (m), PSM07566 (m), PSM07568 (m); Cecil, 6 mi. SE McIntyre Camp (45.56°, –119.87°), PSM07569 (m); Irrigon, 2 mi. W, 1 mi. S Columbia River, 280 ft (45.90°, –119.53°), UWBM50309 (m); T5N, R26E, Sec. 31, NW1/4 (45.87°, –119.61°), PSM26714 (m); 3.5 mi. W Irrigon, McCormack Ranch (45.90°, –119.56°), OSUFW4940 (m); Umatilla NWR, McCormack Ranch (45.90°, –119.56°), OSUFW6824 (m); *Sherman County;* Kent, 2 mi. W, (45.20°, –120.73°), UWBM47045 (m), UWBM47093 (m); Millers, mouth of Deschutes River (45.63°, –120.90°), USNM206755 (m), USNM206756 (m), USNM206828 (m); *Umatilla County;* Umatilla (45.92°, –119.34°), USNM209210 (m), USNM209212 (m), USNM209211 (m); *Wallowa County;* 15 mi. N Paradise at Horse Creek (45.98°, –117.05°), USNM232325 (m); *Wasco County;* Maupin, 1,063 ft (45.18°, –121.08°), USNM207018 (m); ***Washington;*** *Benton County;* Arid Land Ecology Reserve, 1,200 ft (46.48°, –119.61°), PSM19966 (m), PSM19967 (m), PSM19968 (m), PSM19969 (m), PSM19970 (m), PSM19975 (m), PSM19976 (m),

PSM19977 (m), PSM19978 (m), PSM19979 (m), PSM19980 (m), PSM19981 (m), PSM19982 (m), PSM19983 (m), PSM19984 (m), PSM19986 (m), PSM19990 (m), PSM19992 (m), PSM19993 (m), PSM19971 (m), PSM19972 (m), PSM19973 (m), PSM19974 (m); Columbia River shore opposite Ringold Fish Hatchery (46.72°, –119.49°), PSM20590 (m); Kennewick, 5 mi. W (46.21°, –119.24°), UWBM47137 (m); T5N, R26E, Sec. 13, NE1/4 (45.92°, –119.50°), PSM26724 (m), PSM26725 (m); West end Blalock Island, 250 ft (45.90°, –119.65°), UWBM50319 (m), UWBM50320 (m), UWBM50321 (m), UWBM50323 (m), UWBM50324 (m), UWBM50325 (m), UWBM50326 (m), UWBM50327 (m), UWBM50328 (m), UWBM50329 (m), UWBM50330 (m), UWBM50332 (m), UWBM50333 (m), UWBM50334 (m), UWBM50336 (m), UWBM50337 (m), UWBM50355 (m), UWBM50357 (m), UWBM50359 (m); Whitcomb, 1.5 mi. E, 250 ft (45.87°, –119.75°), UWBM50396 (m), UWBM50397 (m), UWBM50399 (m); *Chelan County;* Entiat Lake, NW shore, 1 mi. SW Chelan Airport (47.86°, –119.96°), PSM20758 (m), PSM20760 (m); *Columbia County;* Starbuck, 645 ft (46.52°, –118.12°), USNM234162 (m); *Douglas County;* 8 mi. N Withrow (47.82°, –119.81°), PSM16309 (m, tail bobbed); 16 mi. N, 5 mi. E Wenatchee, T25N, R21W, Sec. 25 (47.66°, –120.20°), NMMNH3193 (m), NMMNH3194 (m); *Ferry County;* Sanpoil River, W shore, 3 mi. N Roosevelt Lake (48.09°, –118.69°), PSM20764 (m); *Franklin County;* Pasco, 2.5 mi. E, on road from Pasco to Levey (46.24°, –119.05°), UWBM52343 (m), UWBM52344 (m); Pasco, 2.5 mi. ENE, about 0.25 mi. N Levey Road, 500 ft (46.28°, –118.85°), UWBM50394 (m); *Grant County;* across from Vantage, E side of Columbia River, 500 ft (46.95°, –119.96°), UWBM47003 (m); Columbia River, E shore, 10 mi. N Priest Rapids Dam (46.79°, –119.91°), PSM20594 (m); Columbia River, island in, 17 mi. N Wanapum Dam (47.12°, –119.97°), PSM20602 (m); Crab Creek (47.37°, –119.38°), UWBM46998 (m); Frenchman Coulee, 260 m (47.02°, –119.98°), UWBM72490 (m), UWBM72491 (m), UWBM72492 (m), UWBM72493 (m), UWBM72495 (m), UWBM72496 (m), UWBM72497 (m), UWBM72498 (m), UWBM72499 (m); Grand Coulee, 1 mi. NE Brewster Rd. jct. (47.39°, –119.49°), PSM02383 (m); Grand Coulee, Steamboat Rock (47.39°, –119.49°), PSM02404 (m); Moses Lake (47.13°, –119.28°), UWBM47002 (m); Moses Lake, 5 mi. S, 11 mi. W (47.06°, –119.51°), UWBM34409 (m); N. Teal Lake (46.91°, –119.20°), PSM16350 (m); Priest Rapids Dam, 1 mi. N (46.66°, –119.91°), UWBM49929 (m), UWBM49930 (m), UWBM49931 (m); Priest Rapids Dam, 2 mi. N (46.67°, –119.91°), UWBM20533 (m), UWBM49965 (m), UWBM49967 (m), UWBM49969 (m), UWBM49970 (m), UWBM49971 (m); No locality data available, PSM10752 (m), PSM10753 (m), PSM10754 (m), PSM10755 (m), PSM10756 (m), PSM10757 (m); Sun Lakes State Park, 900 ft (47.60°, –119.37°), PSM25784 (m), PSM20141 (m); Wanapum Dam, 17 mi. N, Columbia River island (47.12°, –119.97°), PSM20601 (m); *Kittitas County;* Colockum Pass, T20, R21, Sec. 18, 1,414 m (47.24°, –120.23°), UWBM74016 (m); Colockum Wildlife Area, 2 mi. W Trinidad (47.23°, –120.04°), PSM20598 (m), PSM20599 (m); Columbia River, W shore, opposite Trinidad (47.22°, –120.01°), PSM20600 (m); near Sagebrush Spring (46.89°, –120.07°), UWBM78431 (M, KF382787, KF382885, KF382886, KF382991, KF382992), UWBM78433 (M, KF382788, KF382887, KF382888, KF382993, KF382994); Quilomene Wildlife Recreation Area (47.10°, –120.15°), PSM26509 (m), PSM26510 (m); Saddle Mountain (47.03°, –120.27°), PSM04434 (m); Saddle Mountain, 20 mi. E Ellensburg (47.03°, –120.45°), PSM04430 (m); Saddle Mountain, summit W. Badger Pocket (47.03°, –120.27°), PSM04432 (m); Saddle Mountain, summit, 17 mi. E Ellensburg (47.03°, –120.27°), PSM04429 (m), PSM04433 (m), PSM04435 (m), PSM04436 (m), PSM04437 (m), PSM04438 (m), PSM04439 (m), PSM04440 (m), PSM04441 (m), PSM04442 (m), PSM04444 (m), PSM04445 (m); T17N, R22E, Sec. 8 (46.98°, –120.10°), UWBM34381 (m), UWBM34382 (m), UWBM34383 (m), UWBM34384 (m); *Lincoln County;* (47.43°, –118.73°), UWBM77746 (m); Blue Stem, 1.2 mi. S, 2.3 mi. E, 2,250 ft (47.51°, –118.08°), UWBM51139 (m); Columbia River, S shore, Roosevelt Lake, 1 mi. E Jones Bay Recreation Area (47.93°, –118.59°), PSM20669 (m), PSM20670 (m); (47.53°, –118.47°), UWBM77738 (M, KF382789, KF382889, KF382890, KF382995, KF382996), UWBM77740 (M, KF382790, KF382891, KF382892, KF382997, KF382998); *Okanogan County;* Lake Pateros, E shore opposite SE end Washburn Island (48.08°, –119.66°), PSM20762 (m), PSM20766 (m), PSM20769 (m); Rufus Woods Lake, N shore, 5 mi. N Chief Joseph Dam (48.07°, –119.64°), PSM20771 (m); 1 mi. S, 1.5 mi. W Okanogan, T33N, R26E, Sec. 19 (48.34°, –119.61°), NMMNH3195 (m); 4 mi. S, 3 mi. W Oroville, Wannacut Lake, T39N, R27E (48.88°, –119.50°), NMMNH3278 (m; M, LVT1953, KF382791, KF382893, KF382894, KF382999, KF383000), NMMNH3217 (M, LVT1954, KF382792, KF382895, KF382896, KF383001, KF383002); *Walla Walla County;* along Touchet River (46.30°, –118.33°), UWBM47255 (m); Eureka (46.30°, –118.62°), UWBM46980 (m); Lowden (46.06°, –118.59°), UWBM46979 (m); Touchet River, Prescott, 1 mi. W (46.30°, –118.34°), UWBM47264 (m), UWBM47209 (m); Touchet, 1 mi. W (46.04°, –118.69°), UWBM47182 (m); Touchet, 14 mi. N (46.24°, –118.67°), UWBM47257 (m), UWBM47258 (m); Touchet, 2 mi. N, 5 mi. W (46.70°, –118.78°), UWBM47050 (m), UWBM47051 (m), UWBM47052 (m), UWBM47054 (m), UWBM47056 (m); Touchet, 3 mi. N (46.08°, –118.67°), UWBM47119 (m); Touchet, 7 mi. N (46.14°, –118.67°), UWBM47259 (m); Walla Walla River, 4.5 mi. W Touchet (46.04°, –118.77°), UWBM47153 (m); Wallula (46.09°, –118.90°), UWBM46992 (m) UWBM46993 (m); Wallula Junction, 2 mi. N, 1 mi. E (46.09°, –118.89°), UWBM47207 (m); Wallula, 400 ft (46.09°, –118.90°), UWBM46988 (m); Wallula, 5 mi. SW (46.03°, –118.98°), UWBM47271 (m); Wallula, 5 mi. SW (46.03°, –118.98°), UWBM76249 (m); Wallula, 6 mi. NE (46.15°, –118.82°), UWBM47120 (m); Whitman Mission N. H. S. (45.04°, –118.46°), UWBM77865 (m), UWBM77887 (M, KF382793, KF382897, KF382898, KF383003, KF383004), UWBM78891 (M, KF382794, KF382899, KF382900, KF383005, KF383006); *Whitman County;* Ewan (47.12°, –117.74°), UWBM09661 (m); *Yakima County;* 600 ft above Wenas Creek (46.79°, –120.85°), UWBM27988 (m); Clemans Mountain Burn, 36 mi. W Yakima (46.82°, –120.85°), PSM08944 (m), PSM16379 (m); Ellensburg, 20 mi. SW, Wenas Creek Campground (46.91°, –120.81°), UWBM28015 (m).

Twenty-six specimens of uncertain genetic grouping deleted from morphometric analyses.—***UNITED STATES: Oregon;*** *Deschutes County;* Lower Bridge, 6 mi. W Terrebonne, T14S, R12E, Sec. 16 (44.35°, –121.3°), OSUFW4303, OSUFW4305, OSUFW4307, OSUFW4308; between Cloverdale and Cline Falls, Buckhorn Rd., 1.3 mi. N HWY 126, T14S, R12E, Sec. 32 (44.31°, –121.32°), UWBM41847; *Grant County;* 53 mi. N, 1 mi. E Long Creek, Morgrass Pass Creek, 3,800 ft. (44.77°, –119.12°), OSUFW3797; *Harney County;* 17.5 mi. N, 1.5 mi. E Frenchglen, T29S, R31E, Sec. 4 (43.91°, –118.08°), OSUFW6867; *Jefferson County;* 3 mi. S Madras, T11S, R13E, SW1/4 Sec. 36, 3,000 ft. (44.56°, –121.11°), OSUFW6901; 1 mi. N, 1.5 mi. W Opal City, T13S, R12E, NW1/4 Sec. 12, 3,000 ft. (44.48°, –121.22°), OSUFW6902, OSUFW6903; 3

mi. S Madras, T11S, R13E, SE1/4 Sec. 35, 3,000 ft. (44.56°, –121.12°), OSUFW7035, OSUFW7036; Culver, 4 mi. NNW, T11S, R12E, Sec. 25, SW1/4 (44.58°, –121.25°), PSM13073, PSM13074; Dry Creek, T24S, R41E, Sec. 4, NE1/4 (43.51°, –117.70°), PSM22244; Gateway, 1,795 ft. (44.78°, –121.08°), OSUFW1514, USNM207147; White Horse Sink, USNM247778; *Malheur County;* Rockville (43.28°, –117.10°), USNM207894, USNM207895; 2 mi. NW Riverside (43.56°, –118.19°), USNM213836, USNM213837, USNM213838; ***Washington;*** *Grant County;* Mattawa, 3 mi. W, Priest Rapids WRA, E shore Columbia River, 160 m (46.70°, 119.95°), UWBM76817; *Kittitas County;* Vantage, 13 mi. N, Quilomene Bar, W shore Columbia River, 180 m (47.13°, 120.02°), UWBM76798; *Lincoln County;* Lake Roosevelt N.R.A. [4073], 398 m (47.93°, 118.94°), UWBM77927.

Appendix II

Outgroups used in the phylogenetic (*) and divergence dating (#) analyses by tissue (University of Nevada, Las Vegas Tissue Collection [LVT]) number, voucher (New Mexico Museum of Natural History [NMMNH]) number, and GenBank accession number. N/A = no numbers available. *Cytb* = cytochrome *b*; COIII = cytochrome oxidase subunit 3; IRBP = interphotoreceptor retinoid-binding protein; RAG2 = recombination activating gene 2.

Outgroups	LVT no.	NMMNH no.	Accession no.			
			Cytb	COIII	IRBP	RAG2
*Chaetodipus formosus**#	987	2395	AY926387	AY926424	GQ480800	KF383007
*Perognathus amplus**	403	3297	N/A	AY926414	GQ480801	KF383008
*Perognathus fasciatus**#	2525	3240	AY926410	AY926421	GQ480802	KF383009
*Perognathus flavescens**	2527	3242	N/A	AY926422	GQ480803	N/A
Perognathus flavus#	702	N/A	AY926405	AY926417	GQ480821	KF383010
*Perognathus longimembris**#	2191	2978	AY926408	AY926420	GQ480808	KF383011

Appendix III

Character loadings on the first 5 principal components for 15 cranial and 3 external body measurements for 299 specimens of *Perognathus parvus* and 14 specimens of *P. alticolus*.

	Principal component axis				
	1	2	3	4	5
Eigenvalue	6.629	1.835	1.478	1.159	1.104
% total variance	36.8	10.2	8.2	6.4	6.1
Cumulative % variance	36.8	47	55.2	61.7	67.8
Characters					
Total length	0.301542	−0.0271678	−0.330005	−0.170368	−0.245091
Tail length	0.225163	−0.128385	−0.402107	−0.219623	−0.330949
Hind-foot length	0.211587	0.137321	−0.282075	−0.236463	−0.19931
Length of skull	0.365415	−0.0183321	0.0488523	−0.013155	0.0150591
Skull depth	0.25142	−0.228537	−0.0801271	0.0689862	0.241217
Length of nasals	0.322536	0.102547	0.0768075	0.0198891	−0.0290633
Bulla length	0.192057	−0.558263	0.0184634	0.0607182	0.106155
Length of upper diastema	0.292173	0.106161	0.0407906	0.185941	−0.0528167
Length of maxillary toothrow	0.147057	−0.0835077	0.353522	−0.412786	0.211757
Width of rostrum	0.192558	0.218281	−0.0176421	0.215413	0.420964
Zygomatic breadth	0.316485	0.182396	0.185817	0.0760528	−0.00119886
Least interorbital breadth	0.250321	0.22387	−0.0708688	0.0665431	0.405877
Cranial breadth	0.260314	−0.401694	0.100272	0.0644013	0.0871034
Greatest width of interparietal	0.114175	0.432284	0.24946	0.0868291	−0.265384
Width between P4 and P4	0.0955816	0.0336557	−0.112864	0.550591	−0.224196
Width between M3 and M3	0.0576782	−0.265138	0.428612	0.333729	−0.41116
Length of mandible	0.259836	0.136995	0.0509181	−0.0658221	−0.0623379
Length of mandibular toothrow	0.0909924	0.0384863	0.443808	−0.407045	−0.171334

Appendix IV

Character loadings on the first 2 discriminant function axes for 3 external and 15 cranial measurements for 299 samples of *Perognathus parvus* and 14 samples of *P. alticolus*.

	Discriminant function axis	
	I	II
Eigenvalue	1.3655	0.32173
% total variance	80.93	19.07
χ^2	343.6945	84.1
d.f.	36	17
P-value	0.00	0.00
Characters		
Total length	0.169216	0.41254
Tail length	−0.0663499	−0.242049
Hind-foot length	0.217737	0.376038
Length of skull	−0.171915	0.393105
Skull depth	0.325653	0.122425
Length of nasals	0.0909302	0.190828
Bulla length	−0.438149	0.367087
Length of upper diastema	0.0141103	−0.0973294
Length of maxillary toothrow	−0.350698	0.163431
Width of rostrum	0.597557	−0.384405
Zygomatic breadth	−0.0585571	−0.973254
Least interorbital breadth	0.339507	0.371718
Cranial breadth	−0.0974521	−0.0672047
Greatest width of interparietal	0.0843666	−0.163357
Width between P4 and P4	0.254282	0.118473
Width between M3 and M3	−0.400282	−0.0975409
Length of mandible	0.231754	−0.0714607
Length of mandibular toothrow	−0.110586	−0.0984472